Available online at www.sciencedirect.com
ScienceDirect
Tetrahedron
Tetrahedron 63 (2007) 6587–6602

Cu^{I}–Fesulphos complexes: efficient chiral catalysts for asymmetric 1,3-dipolar cycloaddition of azomethine ylides

Silvia Cabrera,[a] Ramón Gómez Arrayás,[a] Belén Martín-Matute,[a] Fernando P. Cossío[b] and Juan C. Carretero[a,*]

[a]*Departamento de Química Orgánica, Universidad Autónoma de Madrid, Cantoblanco, 28049 Madrid, Spain*
[b]*Kimika Fakultatea, Euskal Herriko Unibertsitatea, P.K. 1072, San Sebastián-Donostia, Spain*

Received 15 February 2007; revised 14 March 2007; accepted 21 March 2007
Available online 27 March 2007

Abstract—The Cu^{I}–Fesulphos catalyst system ($\leq$3 mol %) shows an excellent performance in the asymmetric 1,3-dipolar cycloaddition of azomethine ylides. High to very high levels of reactivity, *endo*/*exo* selectivity, and enantioselectivity (69–>99% ee) are generally achieved with a very wide range of azomethine ylides and dipolarophiles. Based on experimental and computational studies data, a model that accounts for this high enantiocontrol is proposed.

1. Introduction

The catalytic asymmetric 1,3-dipolar cycloaddition reaction is likely the most straightforward and atom-economical method for the enantioselective synthesis of five-membered ring heterocycles.[1] In recent years a wide variety of dipoles have been successfully applied in asymmetric catalytic cycloadditions, including nitrones,[2] carbonyl ylides,[3] nitrile oxides,[2f,4] diazoalkanes,[5] azomethine imines,[6] nitrile imines,[7] and azomethine ylides.[8] In particular, the synthesis of optically active pyrrolidine derivatives by 1,3-dipolar cycloaddition reaction of azomethine ylides was first reported by Grigg and Allway in 1991[9] using stoichiometric amounts of $CoCl_2$ or $MnBr_2$ and an ephedrine derivative as the chiral catalyst. However, despite its synthetic relevance, the catalytic enantioselective version of this cycloaddition has been developed only recently. Highly enantio- and *endo*-selective reactions of stabilized glycine-derived *N*-metalated azomethine ylides with electron-deficient alkenes have been reported by Jørgensen [Zn^{II}–bisoxazoline (N,N ligand),[10a] or Ag^{I}–cinchona alkaloids[10b]], Zhang [Ag^{I}–bisferrocenyl phosphine amide ligand (N,P ligand)],[11] Schreiber [Ag^{I}–QUINAP (N,P ligand)],[12] Zhou [Ag^{I}–ferrocenyloxazoline, (N,P ligand)],[13] and Li [Ag^{I}–Taniaphos type ligand (N,P ligand)].[14] There are also some reports on enantio- and *exo*-selective reactions, although these are scarce.[15] As a dramatic example of the influence of the Lewis acid catalyst on the stereochemical outcome of the reaction, Hou et al.[15c] described that subtle variations in the nature of the aryl groups on the P atom of the chiral Cu^{I}–P,N-ferrocene catalyst lead to a switch of the diastereoselectivity, a reverse *exo*/*endo*-selectivity being achieved in the reaction with nitroalkenes by using either electron-rich or electron-withdrawing substituent. Despite the number of highly efficient examples, a general drawback of the catalytic systems developed is the limited scope with regard to the dipolarophile, each procedure being specific for a narrow variety of activated alkenes. Therefore, the development of highly reactive and enantioselective catalysts showing compatibility with a broad variety of dipolarophiles and azomethine ylides remains a great challenge.

We have previously described a sterically and electronically tuneable family of bidentate 1,2-disubstituted ferrocenyl ligands[16] bearing phosphorus and sulfur heteroatoms as coordinating groups, and the presence of planar chirality as the only source of asymmetry (Fig. 1). These sulfenylphosphinoferrocenes, named Fesulphos ligands (**1**),[17] have proven to be excellent chiral ligands in a variety of highly enantioselective Pd- and Cu-catalyzed reactions, such as allylic substitution reactions,[17a,b] formal aza-Diels–Alder reactions of *N*-sulfonyl imines,[17c] Diels–Alder reaction,[17d] ring-opening of *meso* heterobicyclic alkenes,[17e,f] and Mannich-type reactions of *N*-sulfonyl imines.[17g] Extending the applicability of Fesulphos ligands in asymmetric catalysis, herein we describe in detail that their silver(I) and copper(I) complexes, especially the latter, function as highly efficient chiral Lewis acids in the 1,3-dipolar cycloaddition of azomethine ylides with electrophilic alkenes, providing very good reactivity, *endo*/*exo* selectivity, and exceptional levels of enantioselectivity (up to >99% ee).[18] Furthermore, in contrast to most of

Keywords: 1,3-Dipolar cycloaddition; Azomethine ylide; Asymmetric catalysis; Chiral ligand; Copper; Enantioselectivity; Dipolarophile.
* Corresponding author. Tel.: +34 91 497 3925; fax: +34 91 497 3966; e-mail: juancarlos.carretero@uam.es

0040–4020/$ - see front matter © 2007 Elsevier Ltd. All rights reserved.
doi:10.1016/j.tet.2007.03.130

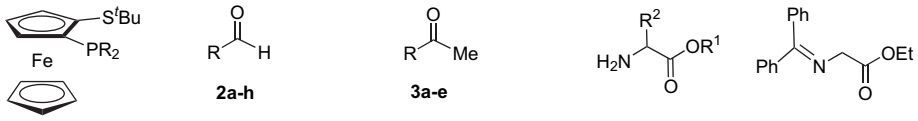

Fesulphos ligands

1a R = Ph
1b R = (*p*-F)C_6H_4
1c R = *o*-Tol
1d R = 1-Naph
1e R = Cy

2a R = Ph
2b R = 1-Naph
2c R = (*p*-F)C_6H_4
2d R = (*p*-OMe)C_6H_4
2e R = (*o*-Me)C_6H_4
2f R = 2-Py
2g R = Cy
2h R = *t*-Bu

3a R = Ph
3b R = (*p*-Cl)C_6H_4
3c R = (*p*-OMe)C_6H_4
3d R = *i*-Pr

4a R^1 = Me, R^2 = H
4b R^1 = *t*-Bu, R^2 = H
4c R^1 = Me, R^2 = Me

Figure 1.

the chiral catalysts reported to date, the Cu^I–Fesulphos system shows a broad scope with regard to the dipolarophile. A mechanistic study based on NMR experiments and theoretical calculations is also provided to rationalize the observed enantioselectivity.

2. Results and discussion

2.1. Preparation of α-imino esters

A wide variety of α-imino esters were readily prepared from reaction of aromatic and aliphatic aldehydes and ketones with different amino esters (Fig. 1).

α-Imino esters derived from aldehydes were prepared following the procedure described in the literature.[19] Thus, reaction of aromatic aldehydes **2a**–**f** with methyl glycinate (**4a**) hydrochloride or *tert*-butylglycinate (**4b**) hydrochloride in CH_2Cl_2 in the presence of Et_3N and $MgSO_4$ at room temperature gave α-imino esters **5a**–**f**, and **6** in good yields (Table 1, entries 1–6 and 9). Similarly, the bulky aliphatic imino esters **5g** and **5h** were prepared by condensation of the corresponding aldehydes (**2g** and **2h**) with methyl glycinate, which was obtained by treatment of methyl glycinate hydrochloride (**4a**) with NH_4OH (Table 1, entries 7 and 8). The lower yields obtained in the case of the aliphatic α-imino esters (24–37%) are likely due to the lower reactivity of their starting aldehydes and, especially, their lower stability. Substituted α-imino esters with an extra methyl group at the α carbon (**7a**–**d**) were prepared from methyl alaninate hydrochloride (**4c**) in good yields (Table 1, entries 10–13). It was also of great interest to study the reactivity of imino esters derived from ketones, a type of azomethine ylides never tested in asymmetric catalytic 1,3-dipolar cycloadditions. The Schiff base derived from benzophenone and ethyl glycinate is commercially available (**8e**). Other α-imino esters derived from ketones were prepared in moderate yield by direct condensation in benzene in the presence of molecular sieves 4 Å. The ketimine **8a**, derived from acetophenone, was obtained in low yield, although it could be easily purified by crystallization in hexane (Table 1, entry 14). The Schiff base derived from *p*-chloroacetophenone (**3b**) was obtained as an inseparable 2.2:1 mixture of ketone (**3b**)/ketimine (**8b**) (Table 1, entry 15), and it was directly used in the cycloaddition reactions. The ketimine derived from *p*-methoxyacetophenone (imine **8c**) could not be purified due to its prompt isomerization to the corresponding enamine (Table 1, entry 16). Finally, the Schiff base derived from the aliphatic ketone **3d** was isolated in 38% yield after evaporation of the remaining starting ketone under low pressure (Table 1, entry 17).

Table 1. Synthesis of α-imino esters **5**, **6**, **7**, and **8**

Entry	Aldehyde/ ketone	α-Amino ester	α-Imino ester	Conditions[a]	Yield[b] (%)
1	**2a**	**4a**	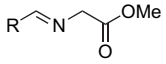 **5a** R = Ph	A	89
2	**2b**	**4a**	**5b**, R=2-Naph	A	84
3	**2c**	**4a**	**5c**, R=(*p*-F)C_6H_4	A	56
4	**2d**	**4a**	**5d**, R=(*p*-OMe)C_6H_4	A	72
5	**2e**	**4a**	**5e**, R=(*o*-Me)C_6H_4	A	80
6	**2f**	**4a**	**5f**, R=2-Py	A	60
7	**2g**	**4a**	**5g**, R=Cy	B	37
8	**2h**	**4a**	**5h**, R=*t*-Bu	B	24
9	**2a**	**4b**	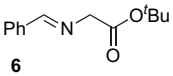 **6**	A	80
10	**2a**	**4c**	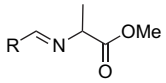 **7a**, R = Ph	A	87
11	**2b**	**4c**	**7b**, R=2-Naph	A	72
12	**2c**	**4c**	**7c**, R=(*p*-OMe)C_6H_4	A	70
13	**2d**	**4c**	**7d**, R=(*o*-Me)C_6H_4	A	73
14	**3a**	**4a**	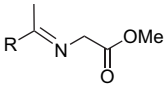 **8a**, R = Ph	C	16 (30)[c]
15	**3b**	**4a**	**8b**, R=(*p*-Cl)C_6H_4	C	—[d]
16	**3c**	**4a**	**8c**, R=(*p*-OMe)C_6H_4	C	—[e]
17	**3d**	**4a**	**8d**, R=*i*-Pr	C	38

[a] Conditions A: Et_3N and $MgSO_4$, in CH_2Cl_2 at room temperature; B: $MgSO_4$, in CH_2Cl_2 at room temperature; C: Molecular sieves 4 Å, benzene at room temperature.
[b] Isolated yield.
[c] In parenthesis, conversion measured by ^1H NMR.
[d] A 2.2:1 mixture of ketone/ketimine was obtained.
[e] A mixture of ketimine/enamine was obtained.

2.2. Asymmetric Fesulphos-catalyzed 1,3-dipolar cycloaddition of azomethine ylides with maleimides

As model reaction we selected the asymmetric 1,3-dipolar cycloaddition of *N*-phenyl maleimide (**9a**) with the α-imino ester **5a** in the presence of catalytic amounts of a base (Et_3N), Fesulphos ligand **1a**, and a metal salt (Table 2). This reaction had been previously studied by Komatsu

Table 2. 1,3-Dipolar cycloaddition of **5a** with maleimides **9a** and **9b**

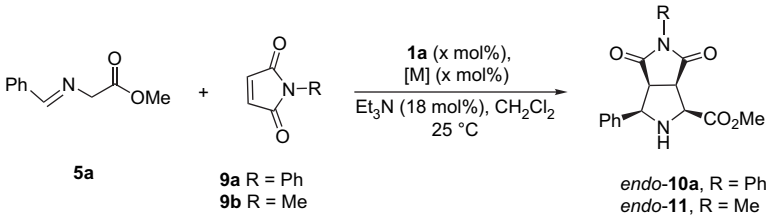

5a

9a R = Ph
9b R = Me

endo-**10a**, R = Ph
endo-**11**, R = Me

Entry	Maleimide	[M]	*X* (mol %)	*t* (h)	*endo*/*exo*[a]	Yield[b] (%)	ee[c] (%)
1	**9a**	CuCl	10	24	94:6	51	30
2	**9a**	$Cu(CH_3CN)_4PF_6$	10	0.25	96:4	74	>99
3	**9a**	$Cu(CH_3CN)_4ClO_4$	10	0.25	>98:<2	78	>99
4	**9a**	$Cu(CH_3CN)_4ClO_4$	1	0.25	95:5	80	>99
5	**9a**	$Cu(CH_3CN)_4ClO_4$	0.5	1	97:3	86	>99
6	**9b**	$Cu(CH_3CN)_4ClO_4$	3	0.25	>98:<2	97	>99
7	**9a**	$AgClO_4$	10	2	96:4	86	89
8	**9a**	AgOAc	10	0.25	>98:<2	64	86
9	**9a**	AgOAc	1	2	>98:<2	90[d]	86
10	**9a**	$Pd(CH_3CN)_2Cl_2$	10	48	96:4	60	0
11[e]	**9a**	$Pd(CH_3CN)_2Cl_2$	10	48	92:8	65	0

[a] Determined by ^{1}H NMR of the crude reaction mixture.
[b] Yield of *endo* product after column chromatographic purification.
[c] Determined by HPLC (Daicel Chiralpak AS-H).
[d] Conversion measured by ^{1}H NMR spectroscopy of the crude reaction mixture.
[e] $AgBF_4$ (20 mol %) was added.

et al. by using $Cu(OTf)_2$/Binap or $Cu(OTf)_2$/Segphos as catalyst system,[15a] describing that under these conditions the reaction occurred at room temperature in 24–48 h with very high *exo*-selectivity, albeit moderate enantioselectivity (up to 72% ee). In contrast to these results, the cycloaddition between **5a** and **9a** catalyzed by CuCl–Fesulphos **1a** (10 mol %) proved to be highly *endo*-selective (*endo*/*exo*= 94:6), yielding *endo*-**10a** with moderate chemical yield and 30% ee (Table 2, entry 1). To our delight, more electrophilic Cu^I complexes, such as $Cu(CH_3CN)_4PF_6$ or $Cu(CH_3CN)_4ClO_4$, improved dramatically the yields (74–78%) and especially the enantioselectivity, affording *endo*-**10a** practically as a single enantiomer (*endo*/*exo*=>94:<6, >99% ee, entries 2 and 3). Furthermore, the reactions took place in very short reaction times (15 min). Due to this very high reactivity, the catalyst loading could be reduced from 10 to 1 mol % without compromising the yield, selectivity or reaction times (entry 4). Similar results were also obtained reducing the catalyst loading to 0.5 mol % (entry 5), which resulted only in slightly longer reaction times (1 h). Nearly complete *endo*-selectivity (*endo*/*exo*=>98:<2) and enantioselectivity (>99% ee) were also obtained in the Cu^I–Fesulphos cycloaddition to *N*-methylmaleimide (entry 6).

Since silver salts (e.g., $AgClO_4$ and AgOAc) have been widely used as Lewis acids in catalytic asymmetric 1,3-dipolar cycloadditions of azomethine ylides,[10b–14] we also studied the Fesulphos-mediated cycloaddition of the model imine **5a** with phenyl maleimide in the presence of a catalytic amount (1–10 mol %) of $AgClO_4$ or AgOAc (entries 7–9). These reactions took place with excellent *endo*-selectivity and good enantioselectivity (86–89% ee), albeit not as high as the Cu^I/Fesulphos-catalyzed process (>99% ee), showing the superiority of the Cu-catalyzed process. Unlike the Cu- and Ag-promoted reactions, the process catalyzed by a palladium Lewis acid, such as $Pd(CH_3CN)_2Cl_2$, was much slower (24 h) and led to racemic *endo*-**10a** (entry 10). An identical result was obtained by using $Pd(CH_3CN)_2Cl_2$ in combination with $AgBF_4$ to facilitate the formation of a more electrophilic palladium complex (entry 11).

Encouraged by the excellent results obtained with the $Cu(CH_3CN)_4ClO_4$/Fesulphos catalyst system, we extended the study of the 1,3-dipolar cycloaddition reaction of *N*-phenyl maleimide to a wide variety of sterically and electronically different α-imino esters derived from aldehydes or ketones (Table 3). Aromatic α-imino esters derived from aldehydes (R^1=H; imines **5a**–**e**) gave excellent results. As in the case of the phenyl α-imino ester **5a** (Table 3, entry 1), the *p*-methoxy and *o*-methyl substituted substrates (**5d** and **5e**) gave cycloadducts *endo*-**10d** and **10e** in good yields and excellent enantioselectivities at room temperature with 1 mol % of catalyst loading (Table 3, entries 7 and 9). Under identical reaction conditions the 2-naphthyl and *p*-fluorophenyl substituted imino esters (**5b** and **5c**) afforded the corresponding pyrrolidines *endo*-**10b** and **10c** with high *endo*-selectivity but moderate enantioselectivity (72 and 84% ee, entries 3 and 5). Fortunately, this loss of asymmetric induction could be overcome by lowering the reaction temperature to −10 °C and increasing the catalyst loading to 3 mol %, resulting in the formation of a single *endo* enantiomer in both cases (>99% ee, entries 4 and 6). In contrast, the heteroaromatic imino ester **5f** (R=2-Py) gave a complex reaction mixture (entry 11), likely due to the basic and/or metal coordinating nature of the pyridyl unit. On the other hand, although the reaction of the aliphatic imino esters **5g** and **5h** was also completely *endo*-selective (entries 12 and 13), the reactivity and the enantioselectivity were much lower than in the case of the aromatic azomethine ylides.

Next we studied the reactivity of C-2 substituted imino esters, a kind of ylide precursor that had been scarcely tested

Table 3. 1,3-Dipolar cycloaddition of a variety of imino esters with *N*-phenyl maleimide (**9a**)

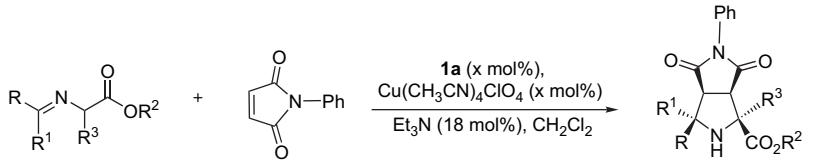

5a-h, R^1 = H, R^2 = Me, R^3 = H
7a-d, R^1 = H, R^2 = Me, R^3 = Me
8a-b,**d**, R^1 = Me, R^2 = Me, R^3 = H
8e, R^1 = Ph, R^2 = Et, R^3 = H

9a

endo-**10a-h**, R^1 = H, R^2 = Me, R^3 = H
endo-**12a-d**, R^1 = H, R^2 = Me, R^3 = Me
endo-**13a-b**,**d**, R^1 = Me, R^2 = Me, R^3 = H
endo-**13e**, R^1 = Ph, R^2 = Et, R^3 = H

Entry	R/Imine	Cu/**1a** (mol %)	*T* (°C)	*t* (h)	Product	*endo*/*exo*[a]	Yield[b] (%)	ee[c] (%)
1	Ph/**5a**	1	25	0.25	**10a**	95:5	80[d]	>99
2	Ph/**5a**	3	−10	0.50	**10a**	>98:<2	81	>99
3	2-Naph/**5b**	1	25	5	**10b**	96:4	63	72
4	2-Naph/**5b**	3	−10	1	**10b**	97:3	81	>99
5	(*p*-F)C_6H_4/**5c**	1	25	5	**10c**	>98:<2	71	84
6	(*p*-F)C_6H_4/**5c**	3	−10	1	**10c**	>98:<2	82	>99
7	(*p*-OMe)C_6H_4/**5d**	1	25	8	**10d**	>98:<2	73[d]	>99
8	(*p*-OMe)C_6H_4/**5d**	3	−10	1	**10d**	>98:<2	81	>99
9	(*o*-Me)C_6H_4/**5e**	1	25	2	**10e**	>98:<2	62	>99
10	(*o*-Me)C_6H_4/**5e**	3	−10	0.50	**10e**	>98:<2	85	>99
11	2-Py/**5f**	3	−10	12	**10f**	—[e]	—	—
12	Cy/**5g**	3	25	24	**10g**	>98:<2	20	40
13	*t*-Bu/**5h**	3	25	24	**10h**	>98:<2	15	51
14	Ph/**7a**	3	−10	48	**12a**	>98:<2	50	80
15	2-Naph/**7b**	3	−10	1	**12b**	>98:<2	78	92
16	(*p*-OMe)C_6H_4/**7c**	3	−10	24	**12c**	>98:<2	<10[f]	ND[g]
17	(*o*-Me)C_6H_4/**7d**	3	−10	24	**12d**	>98:<2	<20[f]	ND[g]
19	Ph/**8a**	3	−10	1	**13a**	>98:<2	78	94
20	(*p*-Cl)C_6H_4/**8b**[h]	3	−10	1	**13b**	>98:<2	80	>99
21	*i*-Pr/**8d**	3	−10	24	**13d**	ND[f]	<15[f]	ND[g]
22	**8e**	3	−10	1	**13e**	>98:<2	92	93

[a] Determined by ^{1}H NMR of the crude reaction mixture.
[b] Yield of *endo* product after column chromatographic purification.
[c] Determined by HPLC (Daicel Chiralpak AS-H or Chiralcel OD).
[d] The yield increased to >96% in the presence of an excess of **5**.
[e] Complex reaction mixture.
[f] Conversion measured by ^{1}H NMR from the crude reaction mixture.
[g] Not determined.
[h] A 2.2:1 mixture of ketone (**2b**)/ketimine (**8b**) was used.

in asymmetric catalytic 1,3-dipolar cycloadditions[12] despite the fact that the addition products are pyrrolidines with a quaternary stereogenic carbon at C-2. The results obtained from a set of four imino esters derived from alanine (R^3=Me, **7a**–**d**) proved to be very dependent on the aryl substitution at the nitrogen atom. Thus, while the cycloaddition of the imino esters **7a** and **7b** occurred with satisfactory yield, complete *endo*-selectivity and high enantioselectivity (80–92% ee, entries 14 and 15), almost no reaction was observed in the case of the imino esters **7c** and **7d** (entries 16 and 17). Finally, we tested the glycinates derived from ketones (imines **8a**–**e**), a kind of azomethines never studied in asymmetric catalytic 1,3-dipolar cycloadditions. The commercially available imine **8e** derived from benzophenone (R=R^1=Ph) provided the pyrrolidine cycloadduct *endo*-**13e** with high enantioselectivity (entry 22, 93% ee). The reactions of the more challenging azomethine ylides derived from acetophenones **8a** and **8b** were also completely *endo*-selective and highly enantioselective (94–>99% ee, entries 19 and 20), giving rise to a single pyrrolidine with a quaternary stereogenic center at C-5 with full control of the four stereogenic centers. Unlike these results, no reaction was observed from the bulky dialkyl imine **8d**, derived from isopropyl methyl ketone (entry 21).

2.3. 1,3-Dipolar cycloaddition of azomethine ylides with other symmetrical 1,2-disubstituted alkenes

Taking into account the stereocontrol achieved by the Cu^I–Fesulphos catalyst system in the reaction with maleimides, we extended the study to other dipolarophiles, starting with other electronically poor symmetrical disubstituted alkenes.

2.3.1. Reaction with dimethyl maleate. While the 1,3-dipolar cycloaddition of azomethine ylides with maleimides catalyzed by Cu^I–Fesulphos or Ag–Fesulphos was highly *endo*-selective, the results obtained with dimethyl maleate were less homogeneous (Table 4). In our first attempt, we used the same reaction conditions to those employed for the cycloaddition of *N*-phenyl maleimide (**9a**). Unlike the behavior of maleimide, the reaction of **5a** and dimethyl maleate (**14**) in CH_2Cl_2 catalyzed by Cu^I/Fesulphos (**1a**)/Et_3N was highly *exo*-selective (*endo*-**15**/*exo*-**15**=10:90, entry 1). The use of diisopropyl ethyl amine (DIPEA) instead of Et_3N gave very similar results (entry 2). The stereoselectivity of this reaction proved to be highly solvent dependent. Thus, in THF or toluene the amount of *endo*-**15** increased dramatically, being the major adduct in THF (entries 3 and 4),

Table 4. 1,3-Dipolar cycloaddition of **5a** with dimethyl maleate (**14**)

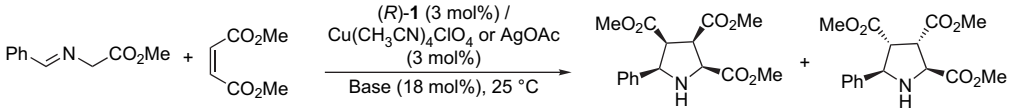

5a **14** *endo*-**15** *exo*-**15**

Entry	[M]	Solvent	Base	T (°C)	**1**	t (h)	*endo*/*exo*[a]	*endo*-**15**		*exo*-**15**	
								Yield[b] (%)	ee[c] (%)	Yield[b] (%)	ee[c] (%)
1	Cu^I	CH_2Cl_2	Et_3N	25	**1a**	48	10:90	—	—	82	23
2	Cu^I	CH_2Cl_2	DIPEA	25	**1a**	24	7:93	—	—	78	21
3	Cu^I	THF	Et_3N	25	**1a**	24	67:33	47	94	32	12
4	Cu^I	THF	DIPEA	25	**1a**	24	67:33	41	94	30	10
5	Cu^I	Toluene	Et_3N	25	**1a**	24	41:59	33	93	59	13
6	Cu^I	CH_3CN	Et_3N	25	**1a**	48	—[d]	—	—	—	—
7	Ag^I	CH_2Cl_2	Et_3N	25	**1a**	24	54:46	36	66	ND[e]	ND[e]
8	Ag^I	THF	Et_3N	25	**1a**	1	85:15	67	68	ND[e]	ND[e]
9	Ag^I	Toluene	Et_3N	25	**1a**	1	90:10	75	67	ND[e]	ND[e]
10	Ag^I	Toluene	Et_3N	−10	**1a**	6	>98:<2	71	75	—	—
11	Ag^I	Toluene	Et_3N	−10	**1b**	6	>98:<2	82	69	—	—
12	Ag^I	Toluene	Et_3N	−10	**1c**	3	66:34	87	79	ND[e]	ND[e]
13	Ag^I	Toluene	Et_3N	−10	**1d**	3	71:29	70	89	ND[e]	ND[e]
14	Ag^I	Toluene	Et_3N	−10	**1e**	3	90:10	80	8	ND[e]	ND[e]

[a] Determined by ^1H NMR of the crude reaction mixture.
[b] Yield of the pure product after column chromatographic purification.
[c] Determined by HPLC (Daicel Chiralpak AS-H).
[d] <20% Conversion by ^1H NMR.
[e] Not determined.

whereas no reaction was observed in acetonitrile (entry 6). It is important to note that both in toluene and THF *endo*-**15** was obtained in very high ee (93–94% ee, entries 3–5), while the *exo* adduct was obtained with very low enantioselectivity (10–13%).

As mentioned in the introduction, silver Lewis acids have been frequently employed in *endo*-selective catalytic asymmetric 1,3-dipolar cycloadditions of azomethine ylides.[10–14] Thus, in an attempt to improve the *endo*-selectivity of the reaction with dimethyl maleate, we turned to the combination AgOAc–Fesulphos (entries 7–14). Unlike the Cu–Fesulphos mediated reaction, in all cases the *endo* adduct was obtained as the major one. A brief study on the effect of the solvent showed that toluene provided the best enantioselectivity (entries 7–9). In particular, by performing the reaction in toluene at −10 °C good *endo*-selectivities were obtained with a variety of Fesulphos ligands (entries 10–14), especially with ligands **1a** and **1b**, whose cycloadditions led exclusively to the *endo* adduct (entries 10 and 11). However, the enantioselectivity of these silver-promoted reactions was significantly lower (66–75% ee with ligand **1a**) than that obtained in the copper-mediated process (93–94% ee). As indicated before, a similar trend was observed in the reaction with *N*-phenyl maleimide (Table 2).

2.3.2. Reaction with dimethyl fumarate and fumaronitrile. Dimethyl fumarate (**16**) showed higher reactivity and *endo*-selectivity[20] than dimethyl maleate (Table 5, entries 1–3). As in the case of dimethyl maleate, the best *endo*-selectivity was achieved in THF, reaching a 90:10 *endo*/*exo* ratio at −10 °C (entry 3). Under these conditions the

Table 5. 1,3-Dipolar cycloaddition of **5a** with dimethyl fumarate (**16**) and fumaronitrile (**17**)

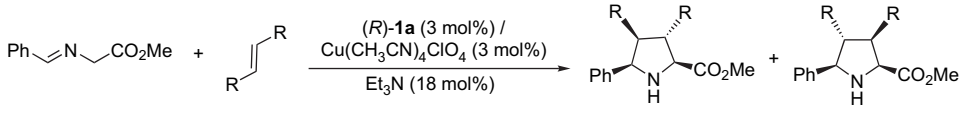

5a **16**, R = CO_2Me; **17**, R = CN *endo*-**18**, R = CO_2Me; *endo*-**19**, R = CN *exo*-**18**, R = CO_2Me; *exo*-**19**, R = CN

Entry	Alkene	Solvent	T (°C)	t (h)	Product	*endo*/*exo*[a]	Yield[b] (%)	ee[c] (%)
1	**16**	CH_2Cl_2	25	24	18	73:27	59	97
2	**16**	THF	25	1	18	88:12	82	>99
3	**16**	THF	−10	5	18	90:10	89	>99
4	**17**	CH_2Cl_2	25	0.25	19	20:80	73	55
5	**17**	THF	25	0.25	19	21:79	71	71
6	**17**	THF	−30	1	19	20:80	78	76

[a] Determined by ^1H NMR of the crude reaction mixtures.
[b] Yield of the major adduct after column chromatographic separation.
[c] Determined by HPLC (Daicel Chiracel OD).

cycloadduct *endo*-**18** was isolated in 89% yield in practically enantiopure form (>99% ee). A very different stereochemical outcome was found in the reaction with fumaronitrile (**17**) (Table 5, entries 4–6). This dipolarophile was quite reactive, allowing to perform the reaction at −30 °C (entry 6), the reaction being moderately *exo*-selective (*endo*/*exo*= 20:80) and enantioselective (up to 76% ee).

2.4. 1,3-Dipolar cycloaddition of azomethine ylides with non-symmetrical alkenes

Extending the scope of the Cu–Fesulphos catalyst system in asymmetric 1,3-dipolar cycloadditions with azomethine ylides, we next undertook the study of a wide variety of monoactivated dipolarophiles, such as methyl acrylate (**20**), 2-butenolide (**22**), methacrolein (**24**), and β-nitrostyrene (**26**). In all cases the cycloadditions occurred with complete regiocontrol (exclusive formation of the 2,4,5-trisubstituted pyrrolidine) and good enantioselectivity (69–95% ee), albeit the *endo*/*exo*-selectivity showed high dependence on the dipolarophile substitution. The most relevant results are shown in Scheme 1.

The reaction with methyl acrylate in THF was moderately *endo*-selective (*endo*/*exo*=75:25), the adduct *endo*-**21** being isolated in 62% yield and 95% ee (Eq. 1). The use of CH_2Cl_2 as solvent or bulkier α,β-unsaturated esters, such as *tert*-butyl acrylate or methyl crotonate, resulted in a sluggish reaction. For instance, the reaction with *tert*-butyl acrylate resulted in 20% conversion after 24 h in THF.

In spite of the chemical interest of the resulting highly functionalized bicyclic pyrrolidines, to the best of our knowledge, α,β-unsaturated lactones had never been tested in asymmetric 1,3-dipolar cycloaddition with azomethine ylides. The Cu–Fesulphos mediated reaction of **5a** with 2-butenolide (**22**) under the usual reaction conditions led to a 60:40 mixture of *endo*/*exo* isomers **23**. After standard silica gel chromatographic separation, *endo*-**23** was isolated in 31% yield in 76% ee. This enantioselectivity could be slightly improved to 80% ee by performing the reaction in CH_2Cl_2 instead of THF (Eq. 2).

Although some examples of catalytic asymmetric 1,3-dipolar cycloadditions of α,β-unsaturated aldehydes with nitrones have been reported,[2h,21] there are no examples of cycloadditions with azomethine ylides. Moreover, the use of α-substituted acroleins would provide a synthetic route to pyrrolidines with a quaternary carbon at C-4. As shown in Eq. 3, the cycloaddition of **5a** with methacrolein (**24**)

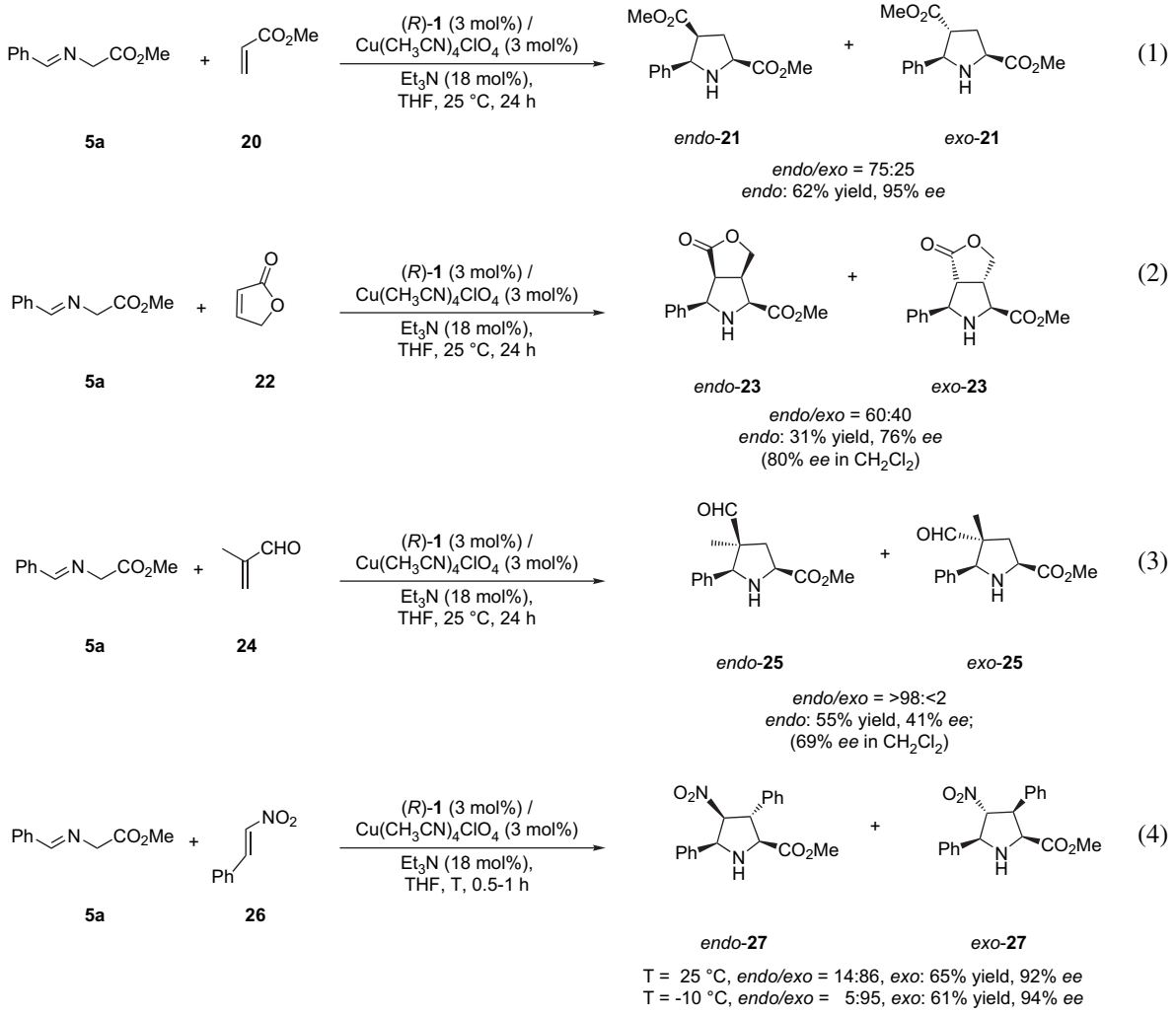

Scheme 1. Catalytic and asymmetric 1,3-dipolar cycloaddition with monoactivated alkenes.

under the standard reaction conditions took place with complete regio- and *endo*-selectivities, albeit the cycloadduct *endo*-**25** was obtained with moderate enantioselectivity (41% ee; Eq. 3). After a brief study of solvents, this asymmetric induction could be improved to 69% ee by performing the reaction in CH_2Cl_2.

The first systematic study on nitroalkenes in catalytic asymmetric 1,3-dipolar cycloadditions with azomethine ylides has been recently reported by Hou et al.[15c] In addition, the group of Cossío has described that pyrrolidines bearing a dipeptide at C-2 and a nitro group at C-4 are potent inhibitors of the enzyme $\alpha_4\beta_1$-integrine, which is involved in the hepatic melanoma metastasis.[22] We were pleased to see that the 1,3-dipolar cycloaddition of (*E*)-β-nitrostyrene (**26**) with the model azomethine ylide precursor **5a** occurred rapidly, providing the C_4-nitro-pyrrolidine adduct **27** with good stereochemical control (Eq. 4). In this case, similar results were obtained in CH_2Cl_2 and THF, although a slightly higher enantioselectivity was achieved in THF. This dipolarophile proved to be very reactive, allowing to perform the reaction at −10 °C (60 min reaction time), leading to the adduct **27** with excellent *exo*-selectivity (*endo*/*exo*=5:95) and enantioselectivity (94% ee).

2.5. Stereochemical assignment of the cycloadducts

The assignment of the *endo*/*exo* configuration of cycloadducts *endo*-**10a**,[11,15a] *endo*-**10d**,[15a] *endo*-**11**,[11,15a] *endo*-**12a**,[23] *endo*-**15**,[11] *endo*-**18**,[10a] *exo*-**19**,[15a] *exo*-**21**,[10a] and *exo*-**27**[24] was made by comparison of their NMR spectroscopic data with those reported in the literature. The configuration of new cycloadducts was assigned assuming a similar reaction pathway, and by 1D and 2D NMR experiments. The study of the ^{1}H NMR data of the maleimide adducts revealed that the *endo* adducts have a big coupling constant for protons H-4 and H-5 ($J_{4,5}$=8–9 Hz), while this value is much lower for the *exo* adducts ($J_{4,5}$= 4–5.5 Hz). A couple of examples is shown in Figure 2.[25] Furthermore, the protons of the methoxy carbonyl group at C-2 are more deshielded for *endo*-**10a** than for *exo*-**10a**. This difference in the chemical shift is likely due to the ring-current effect of the carbonyl group at C-3, which is in a cis relationship with the methoxy carbonyl group in *endo*-**10a**. A similar effect is observed in pyrrolidines with a quaternary carbon, such as *endo*-**12** and *endo*-**13**.

In the case of adducts derived from acyclic dipolarophiles, the chemical shift of the protons of the substituent at C-4 has a great diagnostic value. Thus, this chemical shift is substantially lower for the *endo* adduct (Ph group at C-5 and substituent at C-4 in cis arrangement) than for the *exo* diastereomer, likely due to the shielding ring-current effect of the phenyl group at C-5 on the cis substituent at C-4. For example, the methoxy carbonyl group at C-4 in adduct *endo*-**15**, *endo*-**18**, and *endo*-**21** appears around 0.6 ppm more shielded (3.1–3.2 ppm) than the methoxy carbonyl groups on C-2 and C-3 (at 3.6–3.7 ppm; Fig. 4). Similarly, the signal corresponding to the aldehyde proton of cycloadduct *endo*-**25** also appears at higher field (9.1 ppm) than expected (~9.7 ppm). Additionally, the stereochemical assignment of the new pyrrolidines *endo*-**12a**, *endo*-**13a**, *endo*-**14e**, *endo*-**23**, and *endo*-**25** was confirmed by NOE and NOESY experiments. Figure 3 shows some relevant NOE correlations.

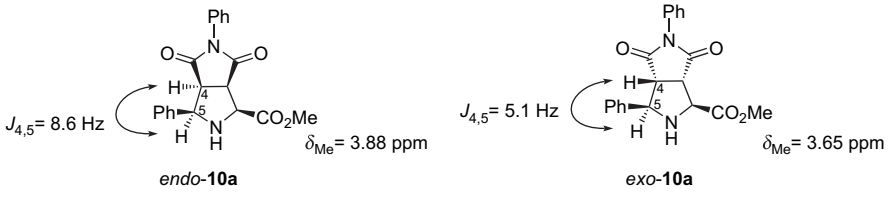

Figure 2.

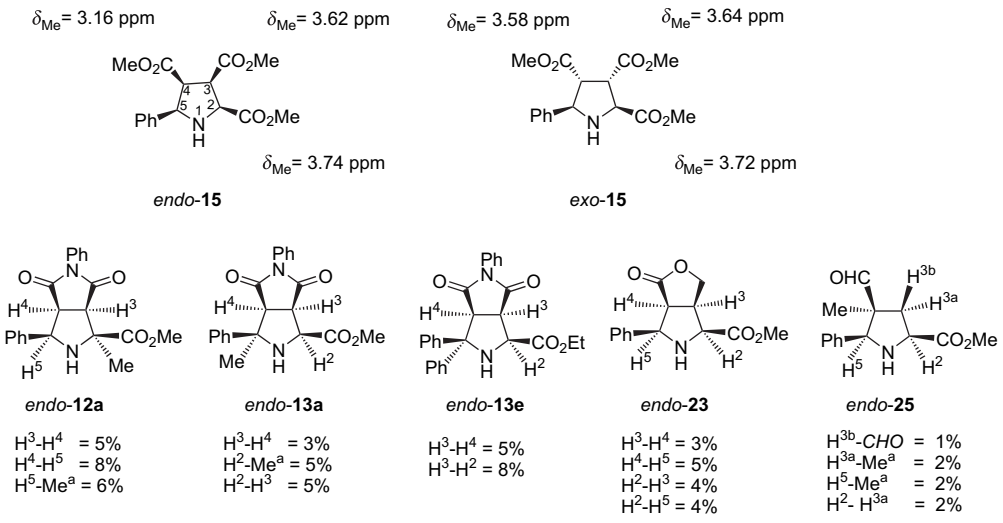

Figure 3.

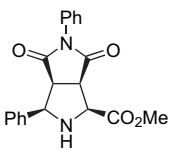

endo-**10a**

$[\alpha]_D^{20}$ +114 (*c* 1.22, CH_2Cl_2); >99% *ee*

Lit. $[\alpha]_D^{20}$ +91.1 (*c* 1.22, CH_2Cl_2); 71% *ee*

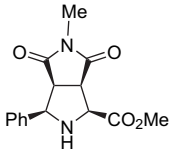

endo-**11**

$[\alpha]_D^{20}$ +51 (*c* 0.14, CH_2Cl_2); >99% *ee*

Lit. $[\alpha]_D^{20}$ +61 (*c* 1.18, CH_2Cl_2); 79% *ee*

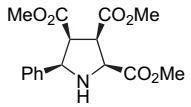

endo-**15**

$[\alpha]_D^{20}$ +100 (*c* 0.05, CH_2Cl_2); 94% *ee*

Lit. $[\alpha]_D^{20}$ +64.7 (*c* 1.07, CH_2Cl_2); 87% *ee*

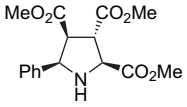

endo-**18**

$[\alpha]_D^{20}$ +43 (*c* 0.10, CH_2Cl_2); >99% *ee*

Lit. $[\alpha]_D^{20}$ +20 (*c* 0.35, CH_2Cl_2); 76% *ee*

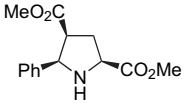

endo-**21**

$[\alpha]_D^{20}$ +36 (*c* 0.08, CH_2Cl_2); 95% *ee*

Lit. $[\alpha]_D^{20}$ +38 (*c* 0.10, CH_2Cl_2); 88% *ee*

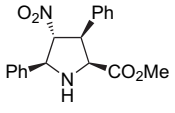

exo-**27**

$[\alpha]_D^{20}$ +105 (*c* 0.11, CH_2Cl_2); 94% *ee*

Lit. $[\alpha]_D^{20}$ +118.2 (*c* 1.10, $CHCl_3$); 97% *ee*

Figure 4.

Finally, the absolute configuration of the cycloadducts was established by comparison of the optical rotation values of (+)-*endo*-**10a**,[11] (+)-*endo*-**11**,[11] (+)-*endo*-**15**,[11] (+)-*endo*-**18**,[10a] (+)-*endo*-**21**,[10a] and (+)-*exo*-**27**[15c] with those reported in the literature (Fig. 4).

2.6. Mechanistic considerations

2.6.1. Isolation of a Fesulphos/Cu/ylide precursor complex. To shed some light on the origin of the excellent enantioselectivity achieved by the Cu–Fesulphos catalyst system in the reaction with a very wide variety of azomethine ylides and dipolarophiles, we first undertook the isolation and characterization of the presumed chiral copper-ligand-imine complex intermediate. Thus, treatment of (*R*)-**1a** with $Cu(CH_3CN)_4ClO_4$ in CH_2Cl_2, followed by addition of **5a** at room temperature, yielded after evaporation of the solvent a relatively stable yellow complex (presumed compound **28**) (Scheme 2).

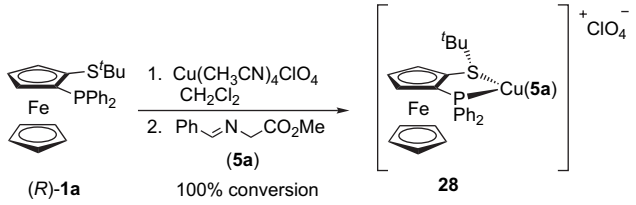

Scheme 2.

The formation of the presumed copper complex **28**, in which the metal atom is simultaneously coordinated with the ligand (*R*)-**1a** and the imine **5a**, is in full agreement with the high deshielding effect observed for the imine and methylene protons of the unit **5a**. Also, the methylene protons of **5a** become an AB system upon coordination with the chiral ligand. Additionally, a significant deshielding effect is also observed for the three protons of the substituted Cp ring of the ligand (Table 6).

Table 6. ^{1}H NMR selected data of **1a**, **5a**, and complex **28** (in $CDCl_3$)

H observed	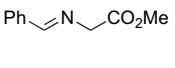 **5a** Shift (ppm)/multiplicity[a]	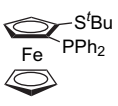 (*R*)-**1a** Shift (ppm)/multiplicity[a]	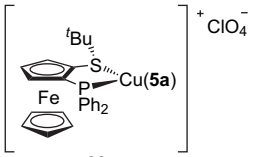 **28** Shift (ppm)/multiplicity[a]
N=C*H*	8.26/s		8.97/s
CH_2	4.39/s		5.11 and 5.08/AB system
CO_2CH_3	3.75/s		3.95/s
Cp-*H*[b]		4.71–4.67/m	4.93/br s
Cp-*H*[b]		4.50–4.46/m	4.81/br s
Cp-*H*[b]		4.15–4.12/m	4.59/br s
Cp′-H_5[c]		3.98/s	3.99/s
$C(CH_3)_3$		1.00/s	1.02/s

[a] s=singlet, br s=broad singlet, and m=multiplet.
[b] Disubstituted cyclopentadienyl ring.
[c] Unsubstituted cyclopentadienyl ring.

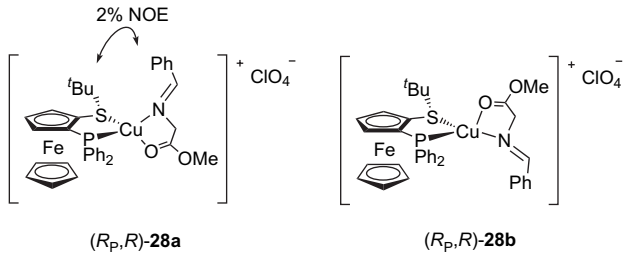

Figure 5.

Based on the X-ray structure of other Fesulphos–Cu^{I} complexes,[17c] we proposed for complex **28** a distorted tetrahedral arrangement of the ligands in the coordination sphere of the Cu atom, and the formation of a single epimer at the sulfur atom, the one with the bulky *t*-Bu group in *anti* relationship with regard to the ferrocene moiety. Two different structures can then be proposed for complex **28**, depending on the orientation of the α-imino ester (**5a**), as shown in Figure 5. Although, unfortunately, suitable crystals for X-ray diffraction analysis could not be obtained, we tentatively proposed the structure **28a** based on the NOE observed between the *t*-Bu group and the protons of the phenyl ring at the imine moiety.

Assuming that **28a** is the chiral metal-complexed ylide precursor involved in the cycloaddition process, the approach of the dipolarophile to its least hindered face (*re* face of the dipole), that avoiding the interaction with the sterically hindered *t*-Bu group, could explain the high enantioselectivity observed in the reaction with most of the dipolarophiles (Scheme 3).

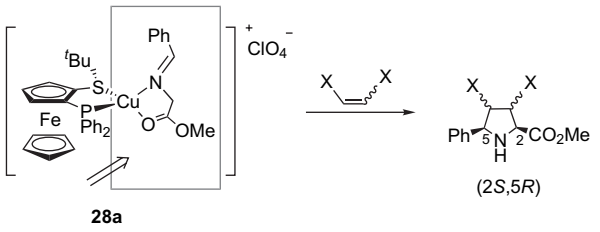

Scheme 3.

2.6.2. Computational studies. In order to gain a better understanding of the structure and reactivity of these complexes, we carried out several computational studies on the Cu and Ag catalysts complexed with the azomethine ylide derived form imino ester **5a**. The fully optimized structures of these complexes, denoted as **29** and **30**, are reported in Figure 6. According to our results, imino ester **5a** can form two diastereomeric silver and copper azomethine ylides in which the metal atoms are coordinated with at least the O and N atoms of the azomethine ylide moiety and the P atom of the catalyst. In the case of Cu complex **29a**, the P–Cu and S–Cu bond distance structures are significantly shorter than those computed for **29b** (Fig. 6). The P–Cu–N and S–Cu–N bond angles are 154 and 113°, respectively.

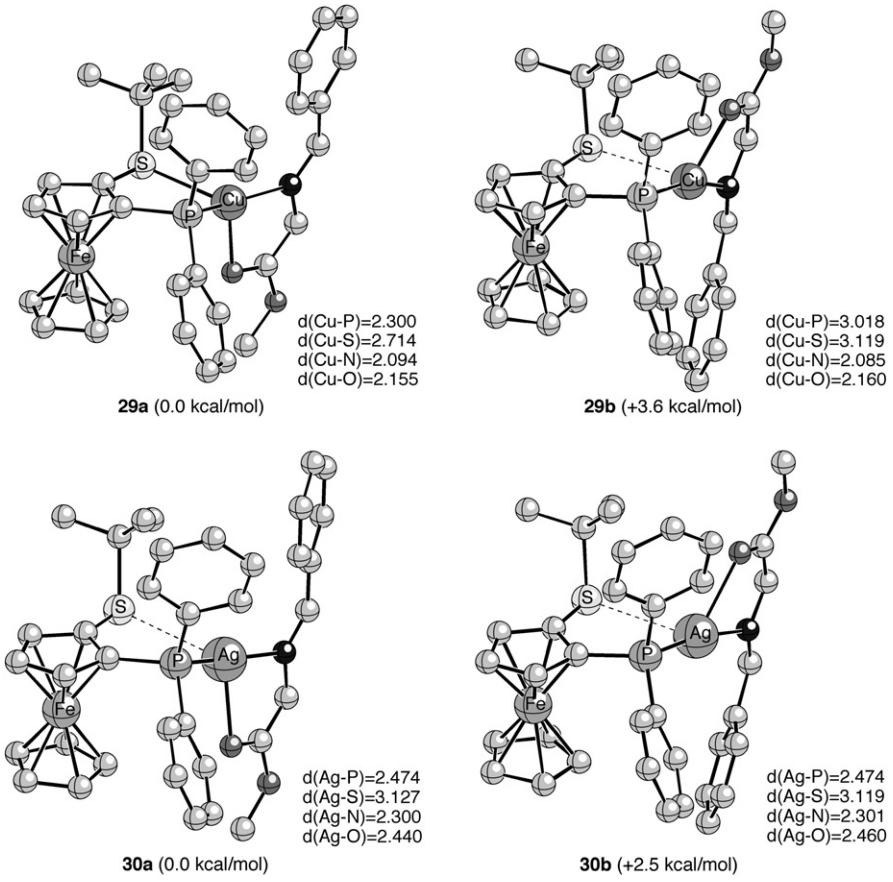

Figure 6. Fully optimized (B3LYP/6-31G* and LANL2DZ level of theory) of complexes **29a** and **29b**, and **30a** and **30b**. Bond distances are given in angstrom. Hydrogen atoms have been omitted for clarity. Numbers in parentheses are the relative energies, calculated at the B3LYP/6-31G* and LANL2DZ-ΔZPVE levels.

In the case of complexes **30a** and **30b**, our calculations suggest that there are no S–Ag covalent bonds, the corresponding Wiberg bond indexes being of only 0.02. Instead, the Natural Bonding Orbital (NBO) analysis indicates that in both cases the interaction between these atoms consists of a two-electron donation between the two lone pairs of the sp^3-hybridized sulfur atom and the empty 5s AO of Ag^I. The second-order perturbational energy associated with these stabilizing donations is of ca. −12.0 kcal/mol. For both complexes, the coordination pattern around the silver atom is T-shaped and the oxygen and nitrogen atoms of the azomethine ylide are in a cis-relationship, the phosphine moiety occupying the distal position with respect to the nitrogen atom.

Complexes **29a** and **30a** are calculated to be 3.6 and 2.5 kcal/mol more stable than **29b** and **30b**, respectively, because in these latter complexes there is a strong steric interaction between the phenyl group of the imine moiety and one of the phenyl groups of the PPh_2 subunit (Fig. 6). In addition, both **29a** and **30a** benefit from a stabilizing electrostatic interaction between the oxygen atom of the azomethine carbonyl group and the iron atom. For instance, in the case of **30a** the O–Fe interatomic distance is 4.772 Å, the corresponding natural charges of the O and Fe atoms being −0.79 and +0.24 a.u., respectively. The computed energy differences indicate that **29a** and **30a** are virtually the exclusive complexes present in the reaction mixtures previous to the cycloaddition steps. These results are in line with those obtained in the previously described NOE experiments (Fig. 5).

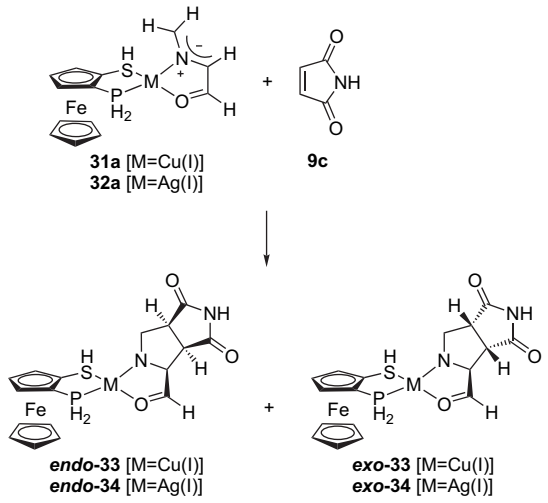

Scheme 4.

Our calculations also indicate that in both complexes one of the faces of the complexed azomethine ylide is closed to further coordination with the dipolarophile because of the high steric congestion imposed by the *tert*-butylsulfenyl subunit linked to the ferrocenyl group. This means that in the major complexes **29a** and **30a** the cycloaddition will take place through the (2*Si*,4*Re*) face and therefore the preferred products will be the cycloadducts indicated in Scheme 3. On the other hand, the shorter distance between the bulky *tert*-butylsulfenyl group and the copper atom in **29a** (distance S–Cu=2.71 Å) compared to that in the silver complex **30a** (distance S–Ag=3.13 Å) would nicely explain the significantly higher enantioselectivity always observed in our copper catalyzed cycloadditions.

The next step in our study was to understand the origins of the high *endo*-selectivity observed in the [3+2] cycloaddtion between imino esters **5** and symmetric cis-dipolarophiles such as maleimides **9a** and **9b**. Given the size of the interacting systems, simplified models such as those gathered in Scheme 4 were studied. The four possible transition structures for the Cu^I and Ag^I complexes **31a** and **32a** to yield the *endo*- and *exo*-cycloadducts **33** and **34** (Scheme 4) are reported in Figure 7.

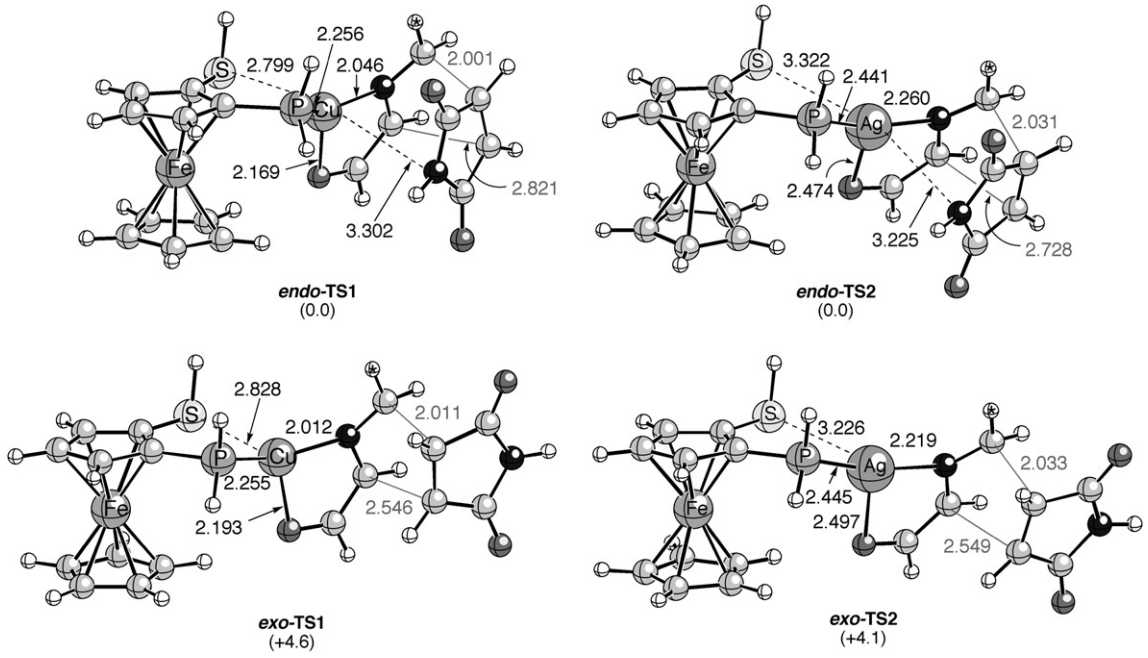

Figure 7. Fully optimized (B3LYP/6-31G* and LANL2DZ level of theory) of *endo* and *exo* transition structures associated with [3+2] cycloadditions depicted in Scheme 3. Bond distances are given in angstrom. Hydrogen atoms have been omitted for clarity. Numbers in parentheses are the relative energies, calculated at the B3LYP/6-31G* and LANL2DZ-ΔZPVE level. The asterisks indicate the position of the susbstituents in azomethine ylides derived form imino esters **5**.

According to our calculations, *endo* transition structures **TS1** and **TS2** lie 4.6 kcal/mol and 4.1 kcal/mol lower in energy than their *exo* analogs, respectively (Fig. 7). These results are in agreement with the nearly complete *endo*-selectivity found for this kind of dipolarophiles (vide supra, Table 3). The reasons for this result cannot be completely attributed to orbital interactions between the dipolarophile and the metallic center. Thus, in *endo*-**TS1** the combined orbital interactions between the maleimide moiety and the Cu atom result in total second-order perturbation energy of ca. −1.5 kcal/mol. In contrast, the N–H moiety of imide **9c** in *endo*-**TS1** exhibits a Coulombic interaction with the Cu atom with an electrostatic energy of −21.5 kcal/mol. The carbonyl groups of the imide moiety also interact with the metallic center, the corresponding electrostatic potential energy being +17.0 kcal/mol. Therefore, the total electrostatic energy between the *endo* imide moiety and the Cu atom is −4.5 kcal/mol, a value in line with the computed relative energies for *endo*- and *exo*-**TS1**. The analysis of *endo*- and *exo*-**TS2** resulted in similar results, thus validating our conclusion that the *endo*-selectivity in this kind of [3+2] cycloadditions is mainly electrostatic in nature. Since Coulombic interactions are very sensitive to substituent and solvent effects, the analysis of the stereochemical outcome with other dipolarophiles will require specific studies in each case.

3. Conclusions

Among different Lewis acids tested, we have found that the combination $Cu(CH_3CN)_4ClO_4$/Fesulphos (0.5–3 mol %) is a very efficient catalyst system for the 1,3-dipolar cycloaddition of azomethine ylides. This catalyst system displays a very high reactivity and provides good yields and stereoselectivities with an exceptionally wide range of dipolarophiles, including diactivated alkenes, such as maleimides, dimethyl maleate, dimethyl fumarate, and fumaronitrile, and monoactivated alkenes, such as α,β-unsaturated esters, methacrolein, and β-nitrostyrene. With the exception of fumaronitrile and β-nitrostyrene, the cycloaddition was *endo*-selective and in all cases good to excellent enantioselectivities were achieved (69–>99% ee). A variety of azomethine ylide precursors derived from methyl glycinate and methyl alaninate were also tested (17 cases), including the first reported examples of catalytic asymmetric 1,3-dipolar cycloadditions of azomethine ylides of ketimines. We have also isolated a presumed Cu–Fesulphos–azomethine complex intermediate and performed some theoretical calculations that shed some light on the origin of the high efficiency of the Cu^I–Fesulphos catalyst system.

4. Experimental

4.1. General methods

All the reactions were carried out in anhydrous solvents and under an argon atmosphere. Melting points were taken in open-end capillary tubes. NMR spectra were recorded at 200 or 300 MHz for ^1H, and at 50 or 75 MHz for ^{13}C, at room temperature in $CDCl_3$ unless stated, using the chloroform residual peaks for calibration (7.26 ppm for ^1H and 77.0 ppm for ^{13}C). The NMR spectra recorded in toluene-d_8 were calibrated using the toluene residual peak (2.09 for ^1H and 20.4 for ^{13}C). Mass spectra (MS) were determined at an ionizing voltage of 70 eV. HPLC experiments were conducted using Daicel Chiralcel OD and Chiralpak AS-H columns. Flash column chromatography was performed using silica gel Merk-60 (230–400 mesh). Ethyl *N*-(diphenylmethylene)glycinate (**8e**) was purchased from Aldrich.

4.1.1. General procedure for the synthesis of α-imino esters (5a–h, 7a–d, and 8a, 8b, and 8d). Method A: To a suspension of the corresponding amino acid ester hydrochloride (23.9 mmol) and $MgSO_4$ (25.0 mmol) in CH_2Cl_2 (25 mL) was added Et_3N (3.4 mL, 23.9 mmol). The mixture was stirred at room temperature for 1 h, and then the corresponding aldehyde (20.0 mmol) was added. The reaction was stirred at room temperature overnight, and the resulting precipitate was removed by filtration. The filtrate was washed with water (15 mL), the aqueous phase was extracted with CH_2Cl_2 (3×10 mL), and the combined organic phases were washed with brine, dried over $MgSO_4$, and concentrated. The resulting imino esters were obtained pure and used in 1,3-dipolar cycloadditions without further purification. Method B: A suspension of methyl glycinate hydrochloride (935 mg, 7.50 mmol) in CH_2Cl_2 (8 mL) was washed with NH_4OH (30%, 5 mL). The organic phase was dried over $MgSO_4$, and filtered. To this solution, $MgSO_4$ (9.94 mmol) and the corresponding aldehyde (5 mmol) were added. The reaction mixture was stirred for 12 h at ambient temperature. After filtration, the organic phase was washed with a saturated solution of NaCl. The aqueous phase was extracted with CH_2Cl_2 (3×10 mL) and the combined organic phases were dried over $MgSO_4$ and concentrated. Method C: A suspension of methyl glycinate hydrochloride (879 mg, 7.00 mmol) in CH_2Cl_2 (8 mL) was washed with NH_4OH (30%, 5 mL). The organic phase was dried over $MgSO_4$, filtered, and concentrated to a final volume of 1 mL. This solution was added to a suspension of the corresponding ketone (6.6 mmol) and MS 4 Å (15 g) in benzene (50 mL). The reaction mixture was stirred for 12 h, filtered, and the solvent evaporated.

4.1.1.1. Methyl (*E*)-*N*-benzylideneglycinate (5a). Yield 89%; ^1H NMR (200 MHz): δ 8.26 (s, 1H, N=CH), 7.77–7.74 (m, 2H, Ar), 7.42–7.39 (m, 3H, Ar), 4.39 (s, 2H, CH_2), 3.75 (s, 3H, CO_2Me).

4.1.1.2. Methyl (*E*)-*N*-(2-naphthylmethylidene)glycinate (5b). Yield 84%; mp: 95–96 °C; ^1H NMR (200 MHz): δ 8.45 (s, 1H, N=CH), 8.10–8.01 (m, 2H, Ar), 7.92–7.85 (m, 3H, Ar), 7.55–7.51 (m, 2H, Ar), 4.48 (s, 2H, CH_2), 3.80 (s, 3H, CO_2Me).

4.1.1.3. Methyl (*E*)-*N*-(*p*-fluorobenzylidene)glycinate (5c). Yield 56%; ^1H NMR (200 MHz): δ 8.26 (s, 1H, N=CH), 7.82–7.74 (m, 2H, Ar), 7.15–7.06 (m, 2H, Ar), 4.40 (s, 2H, CH_2), 3.78 (s, 3H, CO_2Me).

4.1.1.4. Methyl (*E*)-*N*-(*p*-methoxybenzylidene)glycinate (5d). Yield 72%; mp: 67–68 °C; ^1H NMR (200 MHz): δ 8.21 (s, 1H, N=CH), 7.72 (d, *J*=8.8 Hz, 2H, Ar), 6.93 (d, *J*=8.8 Hz, 2H, Ar), 4.38 (s, 2H, CH_2), 3.84 (s, 3H, OMe), 3.77 (s, 3H, CO_2Me).

4.1.1.5. Methyl (*E*)-*N*-(*o*-methylbenzylidene)glycinate (5e). Yield 80%; mp: 50–51 °C; ^1H NMR (200 MHz):

δ 8.60 (s, 1H, N=CH), 7.93 (dd, J=7.5, 1.9 Hz, 1H, Ar), 7.37–7.17 (m, 3H, Ar), 4.44 (s, 2H, CH_2), 3.78 (s, 3H, CO_2Me), 2.52 (s, 3H, Me).

4.1.1.6. Methyl (*E*)-*N*-(2-pyridylmethylidene)glycinate (5f). Yield 72%; ^{1}H NMR (200 MHz): δ 8.66–8.64 (m, 1H, Py), 8.39 (s, 1H, N=CH), 8.08 (d, J=8.0 Hz, 1H, Py), 7.79–7.72 (m, 1H, Py), 7.37–7.31 (m, 1H, Py), 4.47 (s, 2H, CH_2), 3.78 (s, 3H, CO_2Me).

4.1.1.7. Methyl (*E*)-*N*-(cyclohexylmethylidene)glycinate (5g).[26] Yield 37%; ^{1}H NMR (200 MHz): δ 7.49 (d, J=5.1 Hz, 1H, N=CH), 4.15 (s, 2H, CH_2), 3.74 (s, 3H, CO_2Me), 1.86–1.67 (m, 5H, Cy), 1.56–1.21 (m, 6H, Cy).

4.1.1.8. Methyl (*E*)-*N*-(2,2-dimethylpropylidene)glycinate (5h).[26] Yield 24%; ^{1}H NMR (200 MHz): δ 7.55 (s, 1H, N=CH), 4.16 (s, 2H, CH_2), 3.73 (s, 3H, CO_2Me), 1.01 (s, 9H, *t*-Bu).

4.1.1.9. Methyl (*E*)-*N*-benzylidenealaninate (7a). Yield 87%; ^{1}H NMR (200 MHz): δ 8.31 (s, 1H, N=CH), 7.80–7.75 (m, 2H, Ar), 7.44–7.40 (m, 3H, Ar), 4.16 (q, J=6.8 Hz, 1H, CH), 3.74 (s, 3H, CO_2Me), 1.53 (d, J=6.8 Hz, 3H, Me).

4.1.1.10. Methyl (*E*)-*N*-(2-naphthylmethylidene)alaninate (7b). Yield 72%; mp: 73–74 °C; ^{1}H NMR (200 MHz): δ 8.48 (s, 1H, N=CH), 8.10–8.01 (m, 2H, Ar), 7.93–7.84 (m, 3H, Ar), 7.58–7.50 (m, 2H, Ar), 4.23 (q, J=6.7 Hz, 1H, CH), 3.77 (s, 3H, CO_2Me), 1.58 (d, J=6.7 Hz, 3H, Me).

4.1.1.11. Methyl (*E*)-*N*-(*p*-methoxybenzylidene)alaninate (7c). Yield 70%; ^{1}H NMR (300 MHz): δ 8.24 (s, 1H, N=CH), 7.72 (d, J=8.7 Hz, 2H, Ar), 6.92 (d, J=8.8 Hz, 2H, Ar), 4.12 (q, J=6.8 Hz, 1H, CH), 3.84 (s, 3H, OMe), 3.74 (s, 3H, OMe), 1.51 (d, J=6.8 Hz, 3H, Me).

4.1.1.12. Methyl (*E*)-*N*-(*o*-methylbenzylidene)alaninate (7d). Yield 73%; ^{1}H NMR (200 MHz): δ 8.61 (s, 1H, N=CH), 7.93–7.90 (m, 1H, Ar), 7.35–7.15 (m, 3H, Ar), 4.06 (q, J=6.8 Hz, 1H, CH), 3.74 (s, 3H, CO_2Me), 2.50 (s, 3H, *Me*–C_6H_4), 1.53 (d, J=6.8 Hz, 3H, Me).

4.1.1.13. Methyl *N*-(1-phenylethylidene)glycinate (8a). Yield 16%; 30% conversion); mp: 57–58 °C; ^{1}H NMR (200 MHz, C_6D_6): δ 7.97–7.92 (m, 2H, Ar), 7.21–7.17 (m, 3H, Ar), 4.13 (s, 2H, CH_2), 3.44 (s, 3H, CO_2Me), 1.66 (s, 3H, CH_3).

4.1.1.14. Methyl *N*-(1-*p*-chlorophenylethylidene)glycinate (8b). It was obtained as a 2.1:1 mixture of **8b/2b**, and used without further purification; ^{1}H NMR (200 MHz, C_6D_6): δ 7.65 (d, J=8.6 Hz, 2H, Ar), 7.14 (d, J=8.6 Hz, 2H, Ar), 4.07 (s, 2H, CH_2), 3.43 (s, 3H, CO_2Me), 1.53 (s, 3H, Me).

4.1.1.15. Methyl *N*-(1-ethyl-2-methylpropylidene)glycinate (8d). Yield 38%; ^{1}H NMR (200 MHz, C_6D_6): δ 3.96 (s, 2H), 3.39 (s, 3H, CO_2Me), 2.44–2.30 (m, 1H), 1.33 (s, 3H), 1.07 (d, J=6.6 Hz, 6H).

4.1.2. General procedure for the asymmetric 1,3-dipolar cycloaddition of azomethine ylides. To a solution of Fesulphos ligand **1a** (2.7 mg, 0.006 mmol) and $Cu(CH_3CN)_4ClO_4$ (2.0 mg, 0.006 mmol) in CH_2Cl_2 (0.5 mL) or THF (0.5 mL), was successively added a solution of the imine (0.20 mmol) in CH_2Cl_2 (1.0 mL) or THF (0.5 mL), Et_3N (5.0 μL, 0.035 mmol), and the corresponding dipolarophile (0.22 mmol in the case of maleimides **9a** and **9b**, 30 mmol for the remaining dipolarophiles). Once the starting material was consumed as monitored by TLC, the mixture was filtered through Celite, and the filtrate was concentrated to dryness. The residue was analyzed by ^{1}H NMR to determine the *endo*/*exo* ratio and purified by flash chromatography (the eluent is indicated in each case). The ee values were determined by HPLC analysis. Racemic *endo*/*exo* mixtures were obtained as above by using $Cu(CH_3CN)_4ClO_4/PPh_3$ (5 mol %) and $Cu(CH_3CN)_4ClO_4$/*rac*-**1a** (5 mol %) or AgOAc/(±)-Binap (5 mol %) as catalyst system.

4.1.2.1. (1*S*,3*R*,3a*S*,6a*R*)-Methyl-4,6-dioxo-3,5-diphenyl-octahydropyrrole [3,4-*c*]pyrrole-1-carboxylate (*endo*-10a).[11] SiO_2 chromatography: *n*-hexane–EtOAc 1:1; mp=180–181 °C (lit.[11] mp: 160–162 °C). $[\alpha]_D^{20}$ +114 (*c* 1.22, CH_2Cl_2), >99% ee; lit.[11] $[\alpha]_D^{20}$ +91.1 (*c* 1.22, CH_2Cl_2) for a 71% ee sample. HPLC: Daicel Chiralpak AS-H, *i*-PrOH/hexane 50:50, flow rate 0.8 mL/min, t_R: 13.6 min (1*S*,3*R*,3a*S*,6a*R*)-**10a** and 29.2 min (1*R*,3*S*,3a*R*, 6a*S*)-**10a**, 220 nm. ^{1}H NMR (200 MHz): δ 7.50–7.32 (m, 8H), 7.17–7.12 (m, 2H), 4.63 (dd, J=8.6, 5.1 Hz, 1H), 4.16 (dd, J=6.5, 5.1 Hz, 1H), 3.88 (s, 3H), 3.78–3.71 (m, 1H), 3.58 (t, J=8.2 Hz, 1H), 2.55–2.50 (m, 1H).

exo-**10a**: Mp: 139–140 °C (lit.[11] mp: 138–140 °C); ^{1}H NMR (200 MHz): δ 7.55–7.31 (m, 10H), 4.65 (d, J=5.1 Hz, 1H), 4.22 (d, J=4.3 Hz, 1H), 4.07 (dd, J=8.9, 4.3 Hz, 1H), 3.65 (s, 3H), 3.67–3.59 (m, 1H), 2.73 (br s, 1H).

4.1.2.2. (1*S*,3*R*,3a*S*,6a*R*)-Methyl-4,6-dioxo-3-naphthyl-5-phenyl-octahydropyrrole [3,4-*c*]pyrrole-1-carboxylate (*endo*-10b). SiO_2 chromatography: *n*-hexane/EtOAc 1:1; mp: 226–227 °C. $[\alpha]_D^{20}$ +165 (*c* 0.11, CH_2Cl_2), >99% ee. HPLC: Daicel Chiralpak AS-H, *i*-PrOH/hexane 50:50, flow rate 0.8 mL/min, t_R: 16.9 min (1*S*,3*R*,3a*S*,6a*R*)-**10b** and 60.1 min (1*R*,3*S*,3a*R*,6a*S*)-**10b**, 220 nm; ^{1}H NMR (300 MHz): δ 7.98 (s, 1H), 7.88–7.83 (m, 3H), 7.57–7.46 (m, 3H), 7.39–7.28 (m, 3H), 7.15–7.11 (m, 2H), 4.78 (dd, J=8.6, 5.0 Hz, 1H), 4.21 (dd, J=6.4, 5.0 Hz, 1H), 3.92 (s, 3H), 3.80 (t, J=6.4 Hz, 1H), 3.68 (t, J=8.6 Hz, 1H), 2.65–2.62 (m, 1H); ^{13}C NMR (75 MHz): δ 175.1, 173.6, 170.1, 134.3, 133.4, 133.3, 131.6, 129.0, 128.5, 128.2, 128.0, 127.9, 126.3, 126.1, 126.0, 125.6, 125.3, 64.3, 61.9, 52.4, 49.4, 48.4; EIMS *m*/*z* (%): 400 (M^+, 18), 227 (78), 196 (33), 167 (100).

exo-**10b**: Mp: 169–170 °C; ^{1}H NMR (200 MHz): δ 7.89–7.82 (m, 4H), 7.60–7.36 (m, 8H), 4.83 (d, J=5.1 Hz, 1H), 4.28 (d, J=4.1 Hz, 1H), 4.13 (dd, J=8.8, 4.1 Hz, 1H), 3.73 (dd, J=8.8, 5.1 Hz, 1H), 3.60 (s, 3H, CO_2Me), 2.84 (br s, 1H); ^{13}C NMR (75 MHz): δ 176.0, 175.9, 171.9, 137.6, 133.1, 133.0, 131.7, 129.2, 128.8, 128.0, 127.7, 126.5, 126.4, 126.3, 125.2, 124.7, 65.9, 62.7, 52.8, 51.9, 49.1; EIMS *m*/*z* (%): 400 (M^+, 38), 341 (88), 227 (76), 194 (87), 167 (100).

4.1.2.3. (1*S*,3*R*,3a*S*,6a*R*)-Methyl 4,6-dioxo-3-(*p*-fluorophenyl)-5-phenyl-octahydropyrrole [3,4-*c*]pyrrole-1-carboxylate (*endo*-10c). SiO_2 chromatography: *n*-hexane/EtOAc 1:1; mp: 179–180 °C. $[\alpha]_D^{20}$ +118 (*c* 0.11, CH_2Cl_2), >99% ee. HPLC: Daicel Chiralpak AS-H, *i*-PrOH/hexane 50:50, flow rate 0.8 mL/min, t_R: 13.6 min (1*S*,3*R*,3a*S*,6a*R*)-**10c** and 28.5 min (1*R*,3*S*,3a*R*,6a*S*)-**10c**, 220 nm; ^{1}H NMR (300 MHz): δ 7.38–7.23 (m, 5H), 7.09–7.05 (m, 2H), 7.00–6.95 (m, 2H), 4.53 (d, *J*=8.7 Hz, 1H), 4.07 (d, *J*=6.6 Hz, 1H), 3.80 (s, 3H), 3.65 (dd, *J*=7.8, 6.6 Hz, 1H), 3.47 (dd, *J*=8.7, 7.9 Hz, 1H), 2.42 (br s, 1H); ^{13}C NMR (75 MHz): δ 174.9, 173.5, 169.9, 162.6 (d, J_{F-C}=245.5 Hz), 132.4, 131.6, 129.1, 128.8 (d, J_{F-C}=8.2 Hz), 128.6, 128.0, 115.5 (d, J_{F-C}=21.3 Hz), 63.5, 61.8, 52.3, 49.2, 48.1; EIMS *m*/*z* (%): 368 (M^+, 7), 309 (53), 195 (100), 162 (68), 135 (96), 108 (22); Anal. Calcd for $C_{20}H_{17}FN_2O_4$: C, 62.21; H, 4.65; N, 7.60. Found: C, 64.82; H, 4.86; N, 7.23. HRMS Calcd for: $C_{20}H_{18}FN_2O_4$ $(M+H)^+$: 369.1251; found: 369.1263.

exo-**10c**: Mp: 63–64 °C; ^{1}H NMR (300 MHz): δ 7.44–7.18 (m, 7H), 7.02–6.95 (m, 2H), 4.51 (d, *J*=5.4 Hz, 1H), 4.14 (d, *J*=4.1 Hz, 1H), 3.95 (dd, *J*=9.0, 4.5 Hz, 1H), 3.63 (s, 3H), 3.45 (dd, *J*=9.0, 5.7 Hz, 1H), 2.40 (br s, 1H); ^{13}C NMR (75 MHz): δ 175.7, 171.7, 164.1, 160.8, 136.1, 131.6, 129.2, 128.9, 128.4, 126.3, 115.6 (d, J_{F-C}=21.0 Hz), 65.1, 62.4, 52.8, 52.2, 49.1; EIMS *m*/*z* (%): 368 (M^+, 8), 309 (100), 195 (30), 162 (84), 135 (41).

4.1.2.4. (1*S*,3*R*,3a*S*,6a*R*)-Methyl 4,6-dioxo-3-(*p*-methoxyphenyl)-5-phenyl-octahydropyrrole [3,4-*c*]pyrrole-1-carboxylate (*endo*-10d).[15a] SiO_2 chromatography: *n*-hexane/EtOAc 1:1; mp: >200 °C (decomp.) (lit.[15a] (±)-*endo*-**10d** mp: 194–196 °C). $[\alpha]_D^{20}$ +106 (*c* 0.16, CH_2Cl_2), >99% ee. HPLC: Daicel Chiralpak AS-H, *i*-PrOH/hexane 50:50, flow rate 0.8 mL/min, t_R: 18.3 min (1*S*,3*R*,3a*S*,6a*R*)-**10d** and 36.9 min (1*R*,3*S*,3a*R*,6a*S*)-**10d**, 220 nm; ^{1}H NMR (200 MHz): δ 7.45–7.32 (m, 5H), 7.19–7.14 (m, 2H), 6.91–6.87 (m, 2H), 4.58 (dd, *J*=8.6, 5.8 Hz, 1H), 4.13 (dd, *J*=6.4, 4.8 Hz, 1H), 3.87 (s, 3H), 3.79 (s, 3H), 3.73 (t, *J*=6.6 Hz, 1H), 3.53 (t, *J*=8.4 Hz, 1H), 2.49 (br s, 1H).

exo-**10d**: Mp: 117–118 °C (lit.[15a] mp: 133–134 °C); ^{1}H NMR (200 MHz): δ 7.54–7.31 (m, 7H), 6.93–6.87 (m, 2H), 4.57 (d, *J*=5.4 Hz, 1H), 4.19 (d, *J*=4.6 Hz, 1H), 4.04 (dd, *J*=8.9, 4.6 Hz, 1H), 3.80 (s, 3H), 3.67 (s, 3H), 3.55 (dd, *J*=9.0, 5.4 Hz, 1H), 2.67 (br s, 1H).

4.1.2.5. (1*S*,3*R*,3a*S*,6a*R*)-Methyl 4,6-dioxo-3-(*o*-methylphenyl)-5-phenyl-octahydropyrrole [3,4-*c*]pyrrole-1-carboxylate (*endo*-10e). SiO_2 chromatography: *n*-hexane/EtOAc 1:1; mp: 154–155 °C. $[\alpha]_D^{20}$ +136 (*c* 0.11, CH_2Cl_2), >99% ee. HPLC: Daicel Chiralpak AS-H, *i*-PrOH/hexane 50:50, flow rate 0.8 mL/min, t_R: 10.9 min (1*S*,3*R*,3a*S*,6a*R*)-**10e** and 50.5 min (1*R*,3*S*,3a*R*,6a*S*)-**10e**, 220 nm. ^{1}H NMR (300 MHz): δ 7.69–7.63 (m, 1H), 7.38–7.19 (m, 6H), 7.09–7.04 (m, 2H), 4.75–4.73 (m, 1H), 4.16–4.14 (m, 1H), 3.88 (s, 3H), 3.74 (t, *J*=6.2 Hz, 1H), 3.65 (t, *J*=8.6 Hz, 1H), 2.45 (s, 3H); ^{13}C NMR (75 MHz): δ 175.1, 173.3, 170.0, 135.8, 135.3, 131.6, 130.0, 128.9, 128.4, 128.0, 126.1 (2C), 125.3, 61.6, 60.6, 52.3, 48.3, 47.0, 19.4; EIMS *m*/*z* (%): 368 (M^+, 7), 364 (7), 305 (41), 191 (100), 158 (50), 131 (86); Anal. Calcd for $C_{21}H_{20}N_2O_4$: C, 69.22; H, 5.53; N, 7.69. Found: C, 68.82; H, 5.57; N, 7.34.

exo-**10e**: Mp: 138–139 °C; ^{1}H NMR (300 MHz): δ 7.45–7.04 (m, 9H), 4.86 (br s, 1H), 4.10–4.07 (m, 2H), 3.64–3.61 (m, 1H), 3.47 (s, 3H), 2.60–2.50 (m, 1H), 2.38 (s, 3H); ^{13}C NMR (75 MHz): δ 176.4, 176.2, 172.0, 138.2, 136.2, 131.7, 131.1, 129.1, 128.7, 128.0, 126.3, 126.1, 125.4, 62.6, 62.1, 52.7, 50.9, 48.7, 19.6; EIMS *m*/*z* (%): 364 (M^+, 8), 305 (100), 191 (52), 158 (71), 131 (47).

4.1.2.6. (1*S*,3*S*,3a*S*,6a*R*)-Methyl 3-cyclohexyl-(4,6-dioxo)-5-phenyl-octahydropyrrole [3,4-*c*]pyrrole-1-carboxylate (*endo*-10g).[27] SiO_2 chromatography: *n*-hexane/EtOAc 1:1. HPLC: Daicel Chiralpak AS-H, hexane/*i*-PrOH 60:40, flow 0.7 mL/min, t_R: 11.0 min (1*S*,3*S*,3a*S*,6a*R*)-**10g** and 12.9 min (1*R*,3*R*,3a*R*,6a*S*)-**10g**, 210 nm; ^{1}H NMR (300 MHz): δ 7.41–7.30 (m, 3H, Ar), 7.19–7.17 (m, 2H, Ar), 3.93 (d, *J*=8.1 Hz, 1H, H-1), 3.75 (s, 3H, CO_2Me), 3.55 (t, *J*=8.0 Hz, 1H, H-6a), 3.41 (t, *J*=7.4 Hz, 1H, H-3a), 2.90 (dd, *J*=10.1, 7.2 Hz, 1H, H-3), 2.31 (d, *J*=11.2 Hz, 1H, NH), 1.87 (d, *J*=12.3 Hz, 1H, Cy), 1.70–1.59 (m, 3H, Cy), 1.31–0.76 (m, 7H, Cy); ^{13}C NMR (75 MHz): δ 175.1, 174.5, 170.6, 131.7, 129.1, 128.7, 126.5, 68.4, 63.1, 52.5, 49.1, 47.7, 38.4, 31.3, 31.2, 26.3, 25.7, 25.5.

4.1.2.7. (1*S*,3*S*,3a*S*,6a*R*)-Methyl 3-*tert*-butyl-(4,6-dioxo)-5-phenyl-octahydropyrrole [3,4-*c*]pyrrole-1-carboxylate (*endo*-10h).[27] SiO_2 chromatography: *n*-hexane/EtOAc 1:1. HPLC: Daicel Chiralpak AS-H, hexane/*i*-PrOH 80:20, flow 0.8 mL/min, t_R: 14.5 min (1*S*,3*S*,3a*S*,6a*R*)-**10h** and 16.1 min (1*R*,3*R*,3a*R*,6a*S*)-**10h**, 210 nm; ^{1}H NMR (300 MHz): δ 7.41–7.28 (m, 3H), 7.17–7.14 (m, 2H), 3.88 (d, *J*=7.4 Hz, 1H), 3.76 (s, 3H), 3.61 (t, *J*=7.7 Hz, 1H), 3.32 (t, *J*=7.9 Hz, 1H), 3.02 (d, *J*=7.9 Hz, 1H), 2.12 (br s, 1H), 1.09 (s, 9H); ^{13}C NMR (75 MHz): δ 176.0, 174.8, 170.5, 131.8, 129.2, 128.8, 126.5, 73.2, 62.3, 52.4, 50.1, 47.4, 33.0, 27.2; EIMS *m*/*z* (%): 330 (M^+, 1), 273 (100), 94 (71).

4.1.2.8. (1*S*,3*R*,3a*S*,6a*R*)-Methyl 5-methyl-4,6-dioxo-3-phenyl-octahydropyrrole [3,4-*c*]pyrrole-1-carboxylate (*endo*-11).[11,28] SiO_2 chromatography: *n*-hexane/EtOAc 1:1; mp: 166–167 °C (lit.[11] mp: 176–177 °C). $[\alpha]_D^{20}$ +51 (*c* 0.14, CH_2Cl_2), >99% ee; lit.[11] $[\alpha]_D^{20}$ +61.0 (*c* 1.18, CH_2Cl_2) for a 79% ee sample. HPLC: Daicel Chiralcel OD, *i*-PrOH/hexane 50:50, flow rate 0.6 mL/min, t_R: 31.3 min (1*S*,3*R*,3a*S*,6a*R*)-**11** and 36.8 min (1*R*,3*S*,3a*R*,6a*S*)-**11**, 220 nm; ^{1}H NMR (200 MHz): δ 7.37–7.33 (m, 5H), 4.51 (dd, *J*=8.3, 5.4 Hz, 1H), 4.07 (dd, *J*=6.5, 4.4 Hz, 1H), 3.89 (s, 3H), 3.64–3.54 (m, 1H), 3.48–3.39 (m, 1H), 2.89 (s, 3H), 2.44 (br s, 1H).

exo-**11**: Mp: 151–152 °C (lit.[11] mp: 137–139 °C); ^{1}H NMR (300 MHz): δ 7.43–7.28 (m, 5H), 4.52 (d, *J*=5.0 Hz, 1H), 4.09 (d, *J*=4.2 Hz, 1H), 3.92 (dd, *J*=8.8, 4.4 Hz, 1H), 3.66 (s, 3H), 3.49 (dd, *J*=8.8, 5.0 Hz, 1H), 3.06 (s, 3H), 2.67 (br s, 1H).

4.1.2.9. (1*S*,3*R*,3a*S*,6a*R*)-Methyl 1-methyl-4,6-dioxo-3,5-diphenyl-octahydropyrrole [3,4-*c*]pyrrole-1-carboxylate (*endo*-12a).[23,27] SiO_2 chromatography: *n*-hexane/EtOAc 1:1; mp: 199–200 °C. $[\alpha]_D^{20}$ +73 (*c* 0.12, CH_2Cl_2), 80% ee. HPLC: Daicel Chiralcel OD, *i*-PrOH/hexane 50:50, flow rate 0.6 mL/min, t_R: 17.3 min (1*R*,3*S*,3a*R*,6a*S*)-**12a** and 28.4 min (1*S*,3*R*,3a*S*,6a*R*)-**12a**, 210 nm.

^{1}H NMR (300 MHz): δ 7.37–7.18 (m, 8H), 7.01–6.98 (m, 2H), 4.81 (d, J=9.1 Hz, 1H), 3.80 (s, 3H), 3.61 (dd, J=9.1, 7.7 Hz, 1H), 3.37 (d, J=7.6 Hz, 1H), 2.59 (br s, 1H), 1.58 (s, 3H); ^{13}C NMR (75 MHz): δ 174.8, 173.5, 172.7, 136.8, 131.5, 129.0, 128.5, 128.4 (2C), 127.1, 126.0, 67.6, 62.4, 55.7, 52.7, 50.2, 23.9; FABMS *m*/*z* (%): 365 (M+H, 100), 305 (43), 154 (64), 149 (62), 136 (67), 69 (60).

4.1.2.10. (1*S*,3*R*,3a*S*,6a*R*)-Methyl 1-methyl-3-naphthyl-4,6-dioxo-5-phenyl-octahydropyrrole [3,4-*c*]pyrrole-1-carboxylate (*endo*-12b).[27] SiO_2 chromatography: *n*-hexane/EtOAc 1:1; mp: >210 °C (decomp.). $[\alpha]_D^{20}$ +105 (*c* 0.12, CH_2Cl_2), 92% ee. HPLC: Daicel Chiralpak AS-H, *i*-PrOH/hexane 50:50, flow rate 0.7 mL/min, t_R: 13.2 min (1*S*,3*R*,3a*S*,6a*R*)-**12b** and 15.9 min (1*R*,3*S*,3a*R*,6a*S*)-**12b**, 220 nm; ^{1}H NMR (300 MHz): δ 7.84 (s, 1H), 7.77–7.71 (m, 3H), 7.44–7.37 (m, 3H), 7.23–7.18 (m, 3H), 6.96–6.93 (m, 2H), 4.98–4.93 (m, 1H), 3.83 (s, 3H), 3.68 (dd, J=9.1, 7.6 Hz, 1H), 3.41 (d, J=7.6 Hz, 1H), 2.65 (d, J=6.5 Hz, 1H), 1.61 (s, 3H); ^{13}C NMR (75 MHz): δ 174.9, 173.6, 172.8, 134.5, 133.4, 133.3, 131.5, 129.0, 128.4, 128.2, 128.0, 127.8, 126.3, 126.1, 126.0, 125.5, 67.6, 62.4, 55.7, 52.7, 50.1, 23.9; EIMS *m*/*z* (%): 414 (M^+, 17), 355 (84), 241 (100), 208 (40), 181 (96).

4.1.2.11. (1*S*,3*R*,3a*S*,6a*R*)-Methyl 3-methyl-4,6-dioxo-3,5-diphenyl-octahydropyrrole [3,4-*c*]pyrrole-1-carboxylate (*endo*-13a).[27] SiO_2 chromatography: *n*-hexane/EtOAc 1:1; mp: 185–186 °C. $[\alpha]_D^{20}$ +87 (*c* 0.27, CH_2Cl_2), 94% ee. HPLC: Daicel Chiralpak AS-H, *i*-PrOH/hexane 50:50, flow rate 0.7 mL/min, t_R: 11.7 min (1*S*,3*R*,3a*S*,6a*R*)-**13a** and 24.6 min (1*R*,3*S*,3a*R*,6a*S*)-**13a**, 210 nm; ^{1}H NMR (300 MHz): δ 7.70–7.66 (m, 2H), 7.43–7.28 (m, 6H), 6.98–6.95 (m, 2H), 4.45 (t, J=6.7 Hz, 1H), 3.90 (s, 3H), 3.82–3.77 (m, 1H), 3.40 (d, J=7.7 Hz, 1H), 2.41 (d, J=6.5 Hz, 1H), 1.74 (s, 3H); ^{13}C NMR (75 MHz): δ 174.8, 173.7, 170.7, 141.8, 131.4, 129.1, 128.9, 128.4, 128.2, 127.7, 126.2, 126.0, 67.3, 60.0, 56.1, 52.4, 49.4, 29.1; EIMS *m*/*z* (%): 364 (M^+, 10), 349 (100), 305 (81), 191 (67), 158 (71).

4.1.2.12. (1*S*,3*R*,3a*S*,6a*R*)-Methyl 3-(*p*-chlorophenyl)-3-methyl-4,6-dioxo-5-phenyl-octahydropyrrole [3,4-*c*]-pyrrole-1-carboxylate (*endo*-13b).[27] SiO_2 chromatography: *n*-hexane/EtOAc 1:1; mp: >210 °C (decomp.). $[\alpha]_D^{20}$ +151 (*c* 0.16, CH_2Cl_2), >99% ee. HPLC: Daicel Chiralpak AS-H, *i*-PrOH/hexane 50:50, flow rate 0.7 mL/min, t_R: 12.6 min (1*S*,3*R*,3a*S*,6a*R*)-**13b** and 37.8 min (1*R*,3*S*,3a*R*,6a*S*)-**13b**, 220 nm; ^{1}H NMR (300 MHz): δ 7.61–7.58 (m, 2H), 7.36–7.29 (m, 5H), 6.97–6.94 (m, 2H), 4.41 (t, J=6.7 Hz, 1H), 3.87 (s, 3H), 3.77 (t, J=7.7 Hz, 1H), 3.37 (d, J=7.7 Hz, 1H), 2.29 (d, J=6.3 Hz, 1H), 1.68 (s, 3H); ^{13}C NMR (75 MHz): δ 174.7, 173.6, 170.6, 140.5, 133.7, 131.4, 129.0, 128.6, 128.3, 127.8, 126.0, 66.8, 60.0, 55.8, 52.5, 49.0, 29.1.

4.1.2.13. (1*S*,3a*S*,6a*R*)-Ethyl 1-methyl-4,6-dioxo-3,3,5-triphenyl-octahydropyrrole [3,4-*c*]pyrrole-1-carboxylate (*endo*-13e).[27] SiO_2 chromatography: *n*-hexane/EtOAc 1:1; mp: 185–186 °C. $[\alpha]_D^{20}$ +161 (*c* 0.14, CH_2Cl_2), 93% ee. HPLC: Daicel Chiralpak AS-H, *i*-PrOH/hexane 30:70, flow rate 0.8 mL/min, t_R: 12.9 min (1*S*,3a*S*,6a*R*)-**13e** and 19.1 min (1*R*,3a*R*,6a*S*)-**13e**, 220 nm; ^{1}H NMR (300 MHz): δ 7.57–7.54 (m, 2H), 7.46–7.43 (m, 2H), 7.30–7.01 (m, 11H), 4.40–4.29 (m, 1H), 4.23–4.12 (m, 1H), 3.85 (t, J=7.7 Hz, 1H), 3.69 (d, J=7.7 Hz, 1H), 3.12–3.07 (m, 2H), 1.18 (t, J=7.2 Hz, 3H); ^{13}C NMR (75 MHz): δ 174.8, 173.9, 170.2, 144.5, 141.4, 131.7, 129.0, 128.9, 128.5, 128.0, 127.7, 127.6, 127.2, 126.4, 126.3, 73.8, 61.7, 60.3, 53.0, 49.1, 14.1; FABMS *m*/*z* (%): 441 (M+1, 100), 367 (14), 154 (18).

4.1.2.14. (2*S*,3*R*,4*S*,5*R*)-Trimethyl 5-phenylpyrrolidine-2,3,4-tricarboxylate (*endo*-15).[11] SiO_2 chromatography: *n*-hexane/EtOAc 4:1; mp: 94–95 °C (lit.[11] mp: 91–93 °C). $[\alpha]_D^{20}$ +100 (*c* 0.05, CH_2Cl_2), 94% ee; lit.[11] $[\alpha]_D^{20}$ +64.7 (*c* 1.07, CH_2Cl_2) for a 87% ee sample. HPLC: Daicel Chiralpak AS-H, *i*-PrOH/hexane 50:50, flow rate 0.8 mL/min, t_R: 7.1 min (2*S*,3*R*,4*S*,5*R*)-**15** and 12.6 min (2*R*,3*S*,4*R*,5*S*)-**15**, 220 nm; ^{1}H NMR (300 MHz): δ 7.28–7.18 (m, 5H), 4.41 (d, J=6.8 Hz, 1H), 4.09 (d, J=8.9 Hz, 1H), 3.74 (s, 3H), 3.66 (d, J=8.2 Hz, 1H), 3.62 (s, 3H), 3.53–3.48 (m, 1H), 3.29 (br s, 1H), 3.16 (s, 3H).

exo-**15**: ^{1}H NMR (300 MHz): δ 7.39–7.36 (m, 2H), 7.28–7.19 (m, 3H), 4.59 (d, J=7.7 Hz, 1H), 4.30 (d, J=6.1 Hz, 1H), 3.72 (s, 3H), 3.64 (s, 3H), 3.58 (s, 3H), 3.56–3.53 (m, 1H), 3.17 (dd, J=16.8, 7.7 Hz, 1H), 2.55 (br s, 1H).

4.1.2.15. (2*S*,3*S*,4*S*,5*R*)-Trimethyl 5-phenylpyrrolidine-2,3,4-tricarboxylate (*endo*-18).[10a] SiO_2 chromatography: *n*-hexane/EtOAc 4:1. $[\alpha]_D^{20}$ +43 (*c* 0.10, CH_2Cl_2), >99% ee; lit.[10a] $[\alpha]_D^{20}$ +20 (*c* 0.35, CH_2Cl_2) for a 76% ee sample. HPLC: Daicel Chiralcel OD, *i*-PrOH/hexane 30:70, flow rate 0.8 mL/min, t_R: 16.1 min (2*S*,3*S*,4*S*,5*R*)-**18** and 26.6 min (2*R*,3*R*,4*R*,5*S*)-**18**, 210 nm; ^{1}H NMR (200 MHz): δ 7.33–7.27 (m, 5H), 4.65 (d, J=7.8 Hz, 1H), 4.20 (d, J=7.3 Hz, 1H), 3.84 (s, 3H), 3.78 (s, 3H), 3.73–3.52 (m, 2H), 3.20 (s, 3H), 2.76 (br s, 1H).

exo-**18**: ^{1}H NMR (200 MHz): δ 7.49–7.27 (m, 5H), 4.33 (d, J=8.9 Hz, 1H), 4.23 (d, J=8.3 Hz, 1H), 3.81–3.71 (m, 1H), 3.76 (s, 3H), 3.71 (s, 3H), 3.65 (s, 3H), 3.42 (dd, J=8.9, 7.8 Hz, 1H), 2.68 (br s, 1H).

4.1.2.16. (2*S*,3*R*,4*R*,5*R*)-Methyl 3,4-dicyano-5-phenylpyrrolidine-2-carboxylate (*exo*-19).[15a] SiO_2 chromatography: *n*-hexane/EtOAc 4:1; mp: 120–121 °C (lit.[15a] mp: 128–130 °C). $[\alpha]_D^{20}$ +356 (*c* 1.0, CH_2Cl_2), 76% ee. HPLC: Daicel Chiralcel OD, *i*-PrOH/hexane 40:60, flow rate 0.7 mL/min, t_R: 21.9 min (2*S*,3*R*,4*R*,5*R*)-**19** and 28.7 min (2*R*,3*S*,4*S*,5*S*)-**19**, 210 nm; ^{1}H NMR (300 MHz): δ 7.44–7.30 (m, 5H), 4.32 (t, J=8.5 Hz, 1H), 4.22 (t, J=7.3 Hz, 1H), 3.84 (s, 3H), 3.61 (t, J=8.4 Hz, 1H), 3.15 (t, J=8.6 Hz, 1H), 2.73 (br s, 1H).

endo-**19**: ^{1}H NMR (300 MHz): δ 7.45–7.40 (m, 5H), 4.57 (t, J=6.1 Hz, 1H), 4.11 (t, J=6.6 Hz, 1H), 3.81 (s, 3H), 3.65 (dd, J=6.6, 4.3 Hz, 1H), 3.51 (dd, J=6.4, 4.4 Hz, 1H), 2.73 (br s, 1H).

4.1.2.17. (2*S*,4*S*,5*R*)-Dimethyl 5-phenylpyrrolidine-2,4-dicarboxylate (*endo*-21).[10a,11] SiO_2 chromatography: *n*-hexane/EtOAc 4:1. $[\alpha]_D^{20}$ +36 (*c* 0.08, CH_2Cl_2), 95% ee; lit.[10a] $[\alpha]_D^{20}$ +38 (*c* 0.10, CH_2Cl_2) for a 88% ee sample. HPLC: Daicel Chiralpak AS-H, *i*-PrOH/hexane 10:90, flow rate 1.0 mL/min, t_R: 15.0 min (2*S*,4*S*,5*R*)-**21** and 24.5 min (2*R*,4*R*,5*S*)-**21**, 210 nm; ^{1}H NMR (200 MHz): δ 7.27–7.16 (m, 5H), 4.47 (d, J=7.8 Hz, 1H), 3.92 (t,

J=8.1 Hz, 1H), 3.76 (s, 3H), 3.25 (q, J=6.9 Hz, 1H), 3.15 (s, 3H), 2.72 (br s, 1H), 2.35 (dd, J=8.1, 6.9 Hz, 2H).

4.1.2.18. (1*S*,3*R*,3a*S*,6a*R*)-Methyl 3-phenyl-4-(oxo)octahydrocyclopentane [*c*]pyrrol-1-carboxylate (*endo*-23). SiO_2 chromatography: *n*-hexane/EtOAc 5:1; mp: 150–151 °C; ^{1}H NMR (300 MHz): δ 7.36–7.30 (m, 5H), 4.55 (d, J=9.1 Hz, 1H), 4.47 (t, J=9.3 Hz, 1H), 4.15 (dd, J=9.4, 6.8 Hz, 1H), 4.07 (d, J=5.5 Hz, 1H), 3.81 (s, 3H), 3.53–3.43 (m, 1H), 3.26 (t, J=9.1 Hz, 1H), 2.47 (br s, 1H); ^{13}C NMR (75 MHz): δ 175.2, 170.5, 137.4, 128.4, 128.3, 127.3, 69.8, 64.5, 63.0, 52.3, 48.5, 41.1; EIMS *m*/*z* (%): 261 (M^+, 1), 202 (100), 144 (9). HPLC: Daicel Chiralpak AS-H, hexane/*i*-PrOH 50:50, flow rate 0.7 mL/min, t_R: 22.7 min (1*S*,3*R*,3a*S*,6a*R*)-**23** and 25.1 min (1*R*,3*S*,3a*R*,6a*S*)-**23**, 220 nm.

exo-**23**: ^{1}H NMR (200 MHz): δ 7.51–7.28 (m, 5H), 4.57 (d, J=4.2 Hz, 1H), 4.48 (d, J=3.8 Hz, 2H), 3.78 (s, 4H), 3.36–3.14 (m, 2H), 2.57 (br s, 1H).

4.1.2.19. (2*S*,4*S*,5*S*)-Methyl 4-formyl-4-methyl-5-phenylpyrrolidine-2-carboxylate (*endo*-25). SiO_2 chromatography: *n*-hexane/EtOAc 2:1. $[\alpha]_D^{20}$ −8 (*c* 0.36, CH_2Cl_2), 69% ee; ^{1}H NMR (300 MHz): δ 9.16 (s, 1H), 7.40–7.28 (m, 5H), 4.13 (s, 1H), 4.05 (dd, J=9.1, 6.5 Hz, 1H), 3.82 (s, 3H), 2.62 (dd, J=13.4, 6.5 Hz, 1H), 2.01 (dd, J=13.4, 9.1 Hz, 1H), 1.28 (s, 3H); ^{13}C NMR (75 MHz): δ 203.8, 174.0, 136.9, 128.6, 128.2, 127.2, 72.7, 57.9, 55.3, 52.3, 37.3, 19.1; EIMS *m*/*z* (%): 247 (M^+, 8), 177 (65), 117 (100), 106 (32); HRMS Calcd for: $C_{14}H_{17}NO_3$ (M^+): 247.1208; found: 247.1205. HPLC: Daicel Chiralpak AS-H, hexane/*i*-PrOH 70:30, flow rate 0.5 mL/min, t_R: 15.7 min (2*S*,4*S*,5*S*)-**25** and 29.5 min (2*R*,4*R*,5*R*)-**25**, 210 nm.

4.1.2.20. (2*S*,3*S*,4*R*,5*S*)-Methyl 4-nitro-3,5-diphenylpyrrolidine-2-carboxylate (*exo*-27).[15c,24] SiO_2 chromatography: *n*-hexane/EtOAc 4:1; mp: 105–106 °C (lit.[24] (±)-*exo*-**27** mp: 113–115 °C). $[\alpha]_D^{20}$ +105 (*c* 0.11, CH_2Cl_2), 94% ee; lit.[15c] $[\alpha]_D^{20}$ +118.2 (*c* 1.10, $CHCl_3$) for a 97% ee sample. HPLC: Daicel Chiralpak AS-H, *i*-PrOH/hexane 20:80, flow rate 0.4 mL/min, t_R: 25.2 min (2*S*,3*S*,4*R*,5*S*)-**27** and 27.1 min (2*R*,3*R*,4*S*,5*R*)-**27**, 220 nm; ^{1}H NMR (200 MHz): δ 7.56–7.52 (m, 2H), 7.45–7.18 (m, 8H), 5.19 (t, J=8.0 Hz, 1H), 4.73 (d, J=7.8 Hz, 1H), 4.48 (d, J=9.1 Hz, 1H), 4.35 (t, J=7.8 Hz, 1H), 3.26 (s, 3H), 2.71 (br s, 1H).

endo-**27**:[15c,24] ^{1}H NMR (300 MHz): δ 7.42–7.26 (m, 10H), 5.28 (dd, J=6.1, 3.1 Hz, 1H), 4.92 (dd, J=10.9, 6.7 Hz, 1H), 4.22 (d, J=7.4, 3.5 Hz, 1H), 4.12 (d, J=7.2 Hz, 1H), 3.81 (s, 3H), 3.36 (br s, 1H).

4.1.2.21. Cu^I-complex (R_p,*R*)-28. To a solution of **1a** (20.0 mg, 0.044 mmol) and $Cu(CH_3CN)_4ClO_4$ (14.6 mg, 0.044 mmol) in CH_2Cl_2 (1 mL), a solution of **5a** (8.4 mg, 0.044 mmol) in CH_2Cl_2 (0.5 mL) was added under a nitrogen atmosphere at ambient temperature. The reaction mixture was stirred for 30 min and the solvent was evaporated to yield the presumed complex (R_P,*R*)-**28** in quantitative yield (35.7 mg): ^{1}H NMR (300 MHz): δ 8.97 (s, 1H, CH=N), 7.97 (d, J=7.4 Hz, 2H, Ar), 7.81–7.77 (m, 2H, Ar), 7.55–7.23 (m, 9H, Ar), 6.73 (t, J=7.7 Hz, 2H, Ar), 5.11 (part A, AB system, J=20.3 Hz, 1H, CH_2), 5.08 (part B, AB system, J=20.3 Hz, 1H, CH_2), 4.93 (br s, 1H, Cp–H), 4.81 (br s, 1H, Cp–H), 4.59 (br s, 1H, Cp–H), 3.99 (br s, 5H, Cp–H′), 3.95 (br s, 3H, OMe), 1.02 (s, 9H, *t*-Bu).

4.2. Computational studies

All the calculations reported in this paper were performed within Density Functional Theory,[29] using the hybrid three-parameter functional commonly denoted as B3LYP.[30] The standard 6-31G* and LANL2DZ (for Fe, Ag, and Cu atoms) basis sets,[31,32] as implemented in the Gaussian 03[33] suite of programs, were used in all cases. Donor–acceptor interactions were also computed using the Natural Bond Orbital (NBO)[34] method. The energies associated with these two-electron interactions were computed by means of the second-order perturbation energy $\Delta E^{(2)}_{\phi\phi^*}$ according to the following equation:

$$\Delta E^{(2)}_{\phi\phi^*} = -n_\phi \frac{\langle \phi^* | \hat{F} | \phi \rangle^2}{\varepsilon_{\phi^*} - \varepsilon_\phi} \quad (1)$$

where ϕ^* and ϕ are the non-Lewis and Lewis localized orbitals, $\hat{F}$ is the Fock operator, n_ϕ is the occupation of the ϕ localized orbital and ε_{ϕ^*} and ε_ϕ are the respective energies. The stationary points were subjected to harmonic analysis.[35] The relative energies were computed including the zero-point vibrational energy corrections (not scaled).

References and notes

1. For general reviews on 1,3-dipolar cycloadditions, see: (a) *Synthetic Applications of 1,3-Dipolar Cycloaddition Chemistry Towards Heterocycles and Natural Products*; Padwa, A., Pearson, W. H., Eds.; Wiley: New York, NY, 2003; (b) Broggini, G.; Zecchi, G. *Synthesis* **1999**, 905; (c) Gothelf, K. V.; Jørgensen, K. A. *Chem. Rev.* **1998**, *98*, 863; (d) *1,3-Dipolar Cycloaddition Chemistry*; Padwa, A., Ed.; Wiley: New York, NY, 1984.
2. Review: (a) Gothelf, K. V.; Jørgensen, K. A. *Chem. Commun.* **2000**, 1449; For some recent examples, see: (b) Palomo, C.; Oiarbide, M.; Arceo, E.; García, J. M.; López, R.; González, A.; Linden, A. *Angew. Chem., Int. Ed.* **2005**, *44*, 6187; (c) Kano, T.; Hashimoto, T.; Maruoka, K. *J. Am. Chem. Soc.* **2005**, *127*, 11926; (d) Sibi, M. P.; Ma, Z.; Jasperse, C. P. *J. Am. Chem. Soc.* **2005**, *127*, 5764; (e) Suga, H.; Nakajima, T.; Itoh, K.; Kakehi, A. *Org. Lett.* **2005**, *7*, 1431; (f) Sibi, M. P.; Ma, Z.; Itoh, K.; Prabagaran, N.; Jasperse, C. P. *Org. Lett.* **2005**, *7*, 2349; (g) Ashizawa, T.; Ohtsuki, N.; Miura, T.; Ohya, M.; Shinozaki, T.; Ikeno, T.; Yamada, T. *Heterocycles* **2006**, *68*, 1801; (h) Argyropoulos, N. G.; Panagiotidis, T.; Coutouli-Argyropoulou, E.; Raptopoulou, C. *Tetrahedron* **2007**, *63*, 321.
3. (a) Kitagaki, S.; Anada, M.; Kataoka, O.; Matsuno, K.; Umeda, C.; Watanabe, N.; Hashimoto, S. *J. Am. Chem. Soc.* **1999**, *121*, 1417; (b) Doyle, M. P.; Forbes, D. C. *Chem. Rev.* **1998**, *98*, 911.
4. (a) Sibi, M. P.; Itoh, K.; Jasperse, C. P. *J. Am. Chem. Soc.* **2004**, *126*, 5366; (b) Tsuji, M.; Ukaji, Y.; Inomata, K. *Chem. Lett.* **2002**, 1112; (c) Zou, N.; Jiang, B. *J. Comb. Chem.* **2000**, *2*, 6.
5. (a) Kano, T.; Hashimoto, T.; Maruoka, K. *J. Am. Chem. Soc.* **2006**, *128*, 2174; (b) Kanemasa, S.; Tanai, T. *J. Am. Chem. Soc.* **2000**, *122*, 10710.

6. (a) Suárez, A.; Downey, W.; Fu, G. C. *J. Am. Chem. Soc.* **2005**, *127*, 11244; (b) Shintani, R.; Fu, G. C. *J. Am. Chem. Soc.* **2003**, *125*, 10778.
7. Sibi, M. P.; Stanley, L. M.; Jasperse, C. P. J. *J. Am. Chem. Soc.* **2005**, *127*, 8276.
8. Reviews: (a) Nájera, C.; Sansano, J. M. *Angew. Chem., Int. Ed.* **2005**, *44*, 6272; (b) Husinec, S.; Savic, V. *Tetrahedron: Asymmetry* **2005**, *16*, 2047.
9. (a) Allway, P.; Grigg, R. *Tetrahedron Lett.* **1991**, *32*, 5817; (b) Grigg, R. *Tetrahedron: Asymmetry* **1995**, *6*, 2475.
10. (a) Gothelf, A. S.; Gothelf, K. V.; Hazell, R. G.; Jørgensen, K. A. *Angew. Chem., Int. Ed.* **2002**, *41*, 4236; (b) Alemparte, C.; Blay, G.; Jørgensen, K. A. *Org. Lett.* **2005**, *7*, 4569.
11. Longmire, J. M.; Wang, B.; Zhang, X. *J. Am. Chem. Soc.* **2002**, *124*, 13400.
12. Chen, C.; Li, X.; Schreiber, S. L. *J. Am. Chem. Soc.* **2003**, *125*, 10174.
13. Zeng, W.; Zhou, Y.-G. *Org. Lett.* **2005**, *7*, 5055.
14. Zeng, W.; Chen, G.-Y.; Zhou, Y.-G.; Li, Y.-X. *J. Am. Chem. Soc.* **2007**, *129*, 750.
15. (a) Oderaotoshi, Y.; Cheng, W.; Fujitomi, S.; Kasano, Y.; Minakata, S.; Komatsu, M. *Org. Lett.* **2003**, *5*, 5043; (b) Gao, W.; Zhang, X.; Raghunath, M. *Org. Lett.* **2005**, *7*, 4241; (c) Yan, X.-X.; Peng, Q.; Zhang, Y.; Zhang, K.; Hong, W.; Hou, X.-L.; Wu, Y.-D. *Angew. Chem., Int. Ed.* **2006**, *45*, 1979.
16. For a recent review on chiral ferrocene ligands in asymmetric catalysis, see: Gómez Arrayás, R.; Adrio, J.; Carretero, J. C. *Angew. Chem., Int. Ed.* **2006**, *45*, 7674.
17. (a) Priego, J.; García Mancheño, O.; Cabrera, S.; Gómez Arrayás, R.; Llamas, T.; Carretero, J. C. *Chem. Commun.* **2002**, 2512; (b) García Mancheño, O.; Priego, J.; Cabrera, S.; Gómez Arrayás, R.; Llamas, T.; Carretero, J. C. *J. Org. Chem.* **2003**, *68*, 3679; (c) García Mancheño, O.; Gómez Arrayás, R.; Carretero, J. C. *J. Am. Chem. Soc.* **2004**, *126*, 456; (d) García Mancheño, O.; Gómez Arrayás, R.; Carretero, J. C. *Organometallics* **2005**, *24*, 557; (e) Cabrera, S.; Gómez Arrayás, R.; Carretero, J. C. *Angew. Chem., Int. Ed.* **2004**, *43*, 3944; (f) Cabrera, S.; Gómez Arrayás, R.; Alonso, I.; Carretero, J. C. *J. Am. Chem. Soc.* **2005**, *127*, 17938; (g) Salvador Gónzalez, A.; Gómez Arrayás, R.; Carretero, J. C. *Org. Lett.* **2006**, *8*, 2977.
18. For a preliminary communication, see: Cabrera, S.; Gómez Arrayás, R.; Carretero, J. C. *J. Am. Chem. Soc.* **2005**, *127*, 16394.
19. For the synthesis of aryl- and alkylimino esters, see: Cooper, D. M.; Grigg, R.; Hargreaves, S.; Kennewell, P.; Redpath, J. *Tetrahedron* **1995**, *51*, 7791.
20. For trans alkenes, *endo* refers to the cycloadduct with the electron-withdrawing group at C-4 and the aromatic groups at C-5 are cis to each other. Similarly, *exo* refers to the cycloadduct where the same groups are trans to each other.
21. For 1,3-dipolar cycloadditions of nitrones with acroleins, see: (a) Carmona, D.; Lamata, M. P.; Viguri, F.; Rodríguez, R.; Oro, L. A.; Balana, A. I.; Lahoz, F. J.; Tejero, T.; Merino, P.; Franco, S.; Montesa, I. *J. Am. Chem. Soc.* **2004**, *126*, 2716; (b) Kano, T.; Hashimoto, T.; Maruoka, K. *J. Am. Chem. Soc.* **2005**, *127*, 11926.
22. Zubia, A.; Mendoza, L.; Vivanco, S.; Aldaba, E.; Carrascal, T.; Lecea, B.; Arrieta, A.; Zimmerman, T.; Vidal-Vanaclocha, F.; Cossío, F. P. *Angew. Chem., Int. Ed.* **2005**, *44*, 2903.
23. Amornraksa, K.; Grigg, R.; Guranatne, H. Q. N.; Kemp, J.; Sridharan, V. *J. Chem. Soc., Perkin Trans. 1* **1987**, 2285.
24. Vivanco, S.; Lecea, B.; Arrieta, A.; Prieto, P.; Morao, I.; Linden, A.; Cossío, F. P. *J. Am. Chem. Soc.* **2000**, *122*, 6078.
25. A similar behaviour was observed in related cycloadducts. See for example: Woller, P. B.; Cromwell, N. H. *J. Org. Chem.* **1970**, *35*, 888.
26. Due to the low stability of **5g** and **5h**, they have to be immediately used after preparation.
27. The racemic reaction using $Cu(CH_3CN)_4ClO_4/PPh_3$ (5 mol %) or $Cu(CH_3CN)_4ClO_4$/*rac*-**1a** (5 mol %) only yielded *endo* adduct.
28. Tsuge, O.; Kanemasa, S.; Yoshioka, M. *J. Org. Chem.* **1988**, *53*, 1384.
29. Parr, R. G.; Yang, W. *Density-Functional Theory of Atoms and Molecules*; Oxford: New York, NY, 1989.
30. (a) Kohn, W.; Becke, A. D.; Parr, R. G. *J. Phys. Chem.* **1996**, *100*, 12974; (b) Becke, A. D. *J. Chem. Soc.* **1993**, *98*, 5648; (c) Becke, A. D. *Phys. Rev. A* **1988**, *38*, 3098.
31. Hehre, W. J.; Radom, L.; Schleyer, P. v. R.; Pople, J. A. *Ab initio Molecular Orbital Theory*; Wiley: New York, NY, 1986; pp 76–87 and references therein.
32. Hay, P. J.; Wadt, W. R. *J. Chem. Phys.* **1985**, *82*, 299.
33. Frisch, M. J.; Trucks, G. W.; Schlegel, H. B.; Scuseria, G. E.; Robb, M. A.; Cheeseman, J. R.; Montgomery, J. A., Jr.; Vreven, T.; Kudin, K. N.; Burant, J. C.; Millam, J. M.; Iyengar, S. S.; Tomasi, J.; Barone, V.; Mennucci, B.; Cossi, M.; Scalmani, G.; Rega, N.; Petersson, G. A.; Nakatsuji, H.; Hada, M.; Ehara, M.; Toyota, K.; Fukuda, R.; Hasegawa, J.; Ishida, M.; Nakajima, T.; Honda, Y.; Kitao, O.; Nakai, H.; Klene, M.; Li, X.; Knox, J. E.; Hratchian, H. P.; Cross, J. B.; Bakken, V.; Adamo, C.; Jaramillo, J.; Gomperts, R.; Stratmann, R. E.; Yazyev, O.; Austin, A. J.; Cammi, R.; Pomelli, C.; Ochterski, J. W.; Ayala, P. Y.; Morokuma, K.; Voth, G. A.; Salvador, P.; Dannenberg, J. J.; Zakrzewski, V. G.; Dapprich, S.; Daniels, A. D.; Strain, M. C.; Farkas, O.; Malick, D. K.; Rabuck, A. D.; Raghavachari, K.; Foresman, J. B.; Ortiz, J. V.; Cui, Q.; Baboul, A. G.; Clifford, S.; Cioslowski, J.; Stefanov, B. B.; Liu, G.; Liashenko, A.; Piskorz, P.; Komaromi, I.; Martin, R. L.; Fox, D. J.; Keith, T.; Al-Laham, M. A.; Peng, C. Y.; Nanayakkara, A.; Challacombe, M.; Gill, P. M. W.; Johnson, B.; Chen, W.; Wong, M. W.; Gonzalez, C.; Pople, J. A. *Gaussian 03, Revision C.02*; Gaussian: Wallingford, CT, 2004.
34. (a) Reed, A. E.; Curtiss, L. A.; Weinhold, F. *Chem. Rev.* **1988**, *88*, 899; (b) Reed, A. E.; Weinstock, R. B.; Weinhold, F. *J. Chem. Phys.* **1985**, *83*, 735.
35. McIver, J. W., Jr.; Komornicki, A. *J. Am. Chem. Soc.* **1972**, *94*, 2625.